


Spring 1-1-2016

Seismic Vulnerability of Hillside Buildings in Northeast India

Sarah Welsh-Huggins Welsh-Huggins
University of Colorado at Boulder, sjwelshhuggins@gmail.com

Follow this and additional works at: https://scholar.colorado.edu/cven_gradetds

 Part of the [Engineering Commons](#), and the [Geophysics and Seismology Commons](#)

Recommended Citation

Welsh-Huggins, Sarah Welsh-Huggins, "Seismic Vulnerability of Hillside Buildings in Northeast India" (2016). *Civil Engineering Graduate Theses & Dissertations*. 189.
https://scholar.colorado.edu/cven_gradetds/189

This Thesis is brought to you for free and open access by Civil, Environmental, and Architectural Engineering at CU Scholar. It has been accepted for inclusion in Civil Engineering Graduate Theses & Dissertations by an authorized administrator of CU Scholar. For more information, please contact cuscholaradmin@colorado.edu.

Seismic Vulnerability of Hillside Buildings in Northeast India

by

SARAH J. WELSH-HUGGINS

B.S., A.B., Lafayette College, 2012

A thesis submitted to the

Faculty of the Graduate School of the

University of Colorado in partial fulfillment

of the requirement for the degree of

Master of Science

Department of Civil, Environmental and Architectural Engineering

2016

This thesis entitled:

Seismic Vulnerability of Hillside Buildings in Northeast India

written by Sarah J. Welsh-Huggins

has been approved for the Department of Civil, Environmental and Architectural
Engineering

Abbie B. Liel (Chair)

Ross Corotis

Shideh Dashti

Date_____

The final copy of this thesis has been examined by the signatories, and we find that both the content and the form meet acceptable presentation standards of scholarly work in the above mentioned discipline.

ABSTRACT

Welsh-Huggins, Sarah J. (M.S.; Civil, Environmental and Architectural Engineering)

Seismic Vulnerability of Hillside Buildings in Northeast India

Thesis directed by Associate Professor Abbie B. Liel

In northeast India, rapid urbanization and limited available land has led to the construction of multi-story, reinforced concrete frames with masonry infill walls on steep hillsides with weak soils. Recent earthquakes in neighboring regions with similar construction strategies suggest that these buildings may be highly vulnerable to earthquake damage. This thesis analyzes the seismic performance of archetypical hillside reinforced concrete buildings with stepped foundations in Aizawl, Mizoram using the results of incremental dynamic analysis to quantify collapse risk and identify potential failure mechanisms. The findings show that shear critical columns exacerbate structural vulnerabilities created by stepped hillside configurations. In an earthquake, structural failure likely will begin with axial failure of the half-length base columns at the top of the slope, followed by sequential failures in downslope columns. Collapse is predicted to occur from exceedance of column shear capacity in the stories supported by half-length columns on stepped, not flat, foundations. Sensitivity studies of alternative structural and material configurations confirm that the current practice of increasing column dimensions at downslope column lines improves lateral strength, relative to uniform column configurations. In addition, utilizing larger transverse reinforcing bars would change column failure mechanisms and increases collapse margin for the expected seismic hazard. The findings demonstrate that improved column shear capacity and above-code detailing may mitigate the seismic vulnerability of Aizawl's hillside reinforced concrete buildings.

ACKNOWLEDGMENTS

Partial support on this project was provided by the National Science Foundation through grant number 1234503. Any opinions, findings, and conclusions or recommendations expressed in this material are those of the author and do not necessarily reflect the views of the National Science Foundation.

My field work in Aizawl was supported in part by the Mortenson Center for Engineering in Developing Communities at the University of Colorado Boulder. Many thanks to Janise Rodgers for her support and guidance during my time in Aizawl and in our many conversations about this study upon my return. The contributions of Shideh Dashti, William Holmes, Zana Karimi, Hari Kumar, Jenny Ramirez Calderon, Siamak Sattar, Carly Schaeffer, Aurora Smedley, and Rinpuii Tlau were invaluable to this research. I would also like to thank my advisor, Abbie Liel, for her academic and financial support to complete this project in concurrence with my doctoral dissertation. She is a patient and wise mentor and I am grateful to have conducted this thesis under her purview. To my research group, my friends outside of the office, and especially, always, forever to my fiancé Xavi...thank you for your encouragement and love, which have kept me grounded and balanced throughout all of my graduate studies.

To my brother and sister and to my parents, I am an engineer because you inspire me to make this world a better, safer place for all who walk upon it. This thesis is dedicated to you.

TABLE OF CONTENTS

Chapter 1	Introduction.....	1
1.1	Motivation.....	1
1.2	Regional Hazards.....	1
1.3	Socio-Political Context.....	4
1.4	Previous Seismic Risk Assessment.....	6
Chapter 2	Aizawl’s Building Stock.....	7
2.1	Field Work.....	7
2.2	Construction Practices.....	8
2.3	Building Materials.....	10
2.4	Building Designs and Characteristics.....	10
2.5	Foundations and Retaining Walls.....	12
Chapter 3	Literature Review.....	14
3.1	Hillside Buildings.....	14
3.2	Soil-Structure-Interaction Modeling.....	17
Chapter 4	Case Study Buildings.....	19
4.1	Control Building Design.....	19
4.2	Initial Design Sensitivity Study.....	21
4.3	Structural Modeling.....	25
4.4	Foundation Modeling.....	26

Chapter 5	Static Analysis	33
5.1	Initial Design Sensitivity Study Results.....	33
5.2	Refined Design Sensitivity Study through Static analysis	42
Chapter 6	Seismic Risk Assessment	45
6.1	Methodology	45
6.2	Ground Motion Selection.....	45
6.3	Dynamic Analysis.....	47
Chapter 7	Conclusions.....	53
7.1	Limitations	53
7.2	Discussion of Findings.....	53
References	55	

LIST OF TABLES

Table 1. Footing dimensions and detailing for case study building.....	21
Table 2. Variations in structural designs.....	24
Table 3. Variations in soil and footing properties and effect on bearing capacities	24
Table 4. Soil properties used for ShallowFootingGen model in OpenSEES	28
Table 5. Footing properties used for ShallowingFootingGen model in OpenSEES	28
Table 6. Vertical resistance versus loading demand from superstructure and backfill and computed factor of safety.....	31
Table 7. Computed values for the ultimate vertical, passive, and lateral soil capacities	32
Table 8. Fundamental period and maximum base shear values from static pushover analysis	33
Table 9. Structural and material design variations for revised building design variations	43
Table 10. Results of pushover analysis for revised sensitivity study models	44
Table 11. Ground motions selected to represent regional seismic hazard in Aizawl.....	47
Table 12. Median values for collapse capacities (presented at $S_a(T_1)$ and $S_a(T = 1.0s)$) and collapse margin ratio and probability of collapse at maximum considered earthquake shaking intensity, accounting for spectral shape and system uncertainty	50

LIST OF FIGURES

Figure 1. Landslide in Ramhlun neighborhood of Aizawl, June 2014 (photo credit: J. Rodgers).....	2
Figure 2. East-west cross-section showing rupture plane expected to cause scenario event from GHI study from GeoHazards International(2014) based on the work of Seeber et al.(2013).	4
Figure 3. Map of India showing the state of Mizoram and the city of Aizawl (S. Welsh-Huggins)	5
Figure 4. Typical residential building in Aizawl with reinforced concrete frame and masonry infill.....	11
Figure 5. (a) Typical foundation column excavation and (b) building diagram for spread footings (diagram reproduced with permission of Aizawl Municipal Council).....	13
Figure 6. Illustration of control building showing (a) elevation view of building configuration and (b) column and beam dimensions and detailing for case study building (dimensions not to scale).....	20
Figure 7. Elevation view of structural variation with different column dimensions at each floor, design ID 6 in Table 2	23
Figure 8. Elevation view of flat foundation building variation, design ID 12 in Table 2.....	23
Figure 9. Schematic of beam-column elements, joints, and shear/axial springs modeled in OpenSEES (number of fibers shown in cross-section not to scale).....	26
Figure 10. Idealization of beam-on-nonlinear-Winkler foundation model (Raychowdhury & Hutchinson, 2009)	27
Figure 11. Static pushover results for building design variations modeled with fixed base and BNWF, and with and without shear springs in columns	35
Figure 12. Comparison of pushover results into (upslope) and out of hill (downslope) directions	36
Figure 13. Pushover comparison for flat foundation vs. stepped foundation models.....	37
Figure 14. Pushover results for variations in structural configuration.....	38
Figure 15. Comparisons of effect of column sizing increasing upslope and decreasing upslope against pushover loading run into and out of the hill	39
Figure 16. Pushover results for material strength variations.....	40
Figure 17. Effect on pushover results from changing foundation model parameters	41

Figure 18. (a) Pushover results for nonlinear models of all building design variations and (b) interstory drift ratios for column lines in control building, where “Floor Number” refers to lowest floor at an individual column line (*e.g.* 2nd floor is lowest for line C4). 44

Figure 19. Acceleration time-history plot for India-Myanmar ground motion..... 46

Figure 20. Collapse fragility curves for all five hillside building design variations at (a) $S_a(T_1)$ and (b) $S_a(T = 1.0s)$ adjusted for spectral shape and system uncertainty, where dashed line indicates $S_a(T = 1.0s) = 0.40g$, corresponding to seismic hazard for the maximum considered earthquake in Indian Seismic Zone V..... 51

Figure 21. Failure sequence for (a) control building design (ID I) showing upslope to downslope “zippering” associated with axial failures of base columns and (b) for building modeled such that $f'_c = 5.0$ ksi model (ID II), meaning failures concentrate in upslope column lines. 52

Chapter 1 INTRODUCTION

1.1 MOTIVATION

Many communities around the world are faced with the challenge of rising populations and limited undeveloped land for new construction. In the city of Aizawl in northeast India, this problem is amplified by the fact that available land for new construction in the city is on steep, mountain sides and ridges. As a result, new residential construction occurs primarily on unstable, weak slopes. Moreover, excavations for new sites dug under existing building foundations can increase the risk of landslides, exacerbating an already significant risk due to over-saturation of soils during the monsoon season. The city also has a high seismic risk, due to the subduction of the Eurasian tectonic plate beneath the Indian plate (GeoHazards International, 2014; USGS, 2015). As the city continues to grow, it is important to assess the seismic vulnerability of the existing and ever-growing building stock, particularly in the light of the recent 2015 Gorkha (Nepal) and 2016 Manipur (India) earthquakes, which affected neighboring regions. The threefold goals of this thesis are to: 1) quantify the collapse risk of typical multi-story reinforced concrete, mixed-use structures in Aizawl; 2) identify the primary mechanisms of structural failure; and 3), investigate how alternative building configurations (in terms of structural and material properties) change the collapse risk and failure mechanisms.

1.2 REGIONAL HAZARDS

Aizawl experiences significant amounts of rain each year; in the rainiest summer month, the city can receive over 19 inches in precipitation with relative humidity reaching 100% (Government of

Introduction

Mizoram, 2012). The city sits on steep mountains ridges that are prone to frequent landslides, especially during the summer monsoon season. In recent years, landslides have killed dozens of people and destroyed numerous houses (GeoHazards International, 2014). Landslides are common throughout the city, especially in locations where excavation for new buildings undermines the foundations of existing buildings above new construction sites. For example, a landslide occurred in the Electric Veng neighborhood in May of 2014 below an ongoing construction site. In June, 2014, another landslide destroyed another construction site near the Ramhlun Sports Complex (Figure 1). For the most part, the city has been able to deal with large landslides as isolated incidents, but a major earthquake could trigger a series of landslides (GeoHazards International, 2014; Iyengar *et al.*, 2010; MIRSAC, 2005).



Figure 1. Landslide in Ramhlun neighborhood of Aizawl, June 2014 (photo credit: J. Rodgers).

The occurrence of a major earthquake could prove catastrophic for the city. Aizawl sits on top of the Burma Ridges, a large geological belt south of the Himalayas created by the collision of the Indian and Eurasian plates. Below Aizawl, the Eurasian plate is subducting beneath the Indian plate (Figure 2), with the potential to produce a high magnitude earthquake event in the region.

The outcomes of two recent earthquake events in South Asia reinforce concerns about Aizawl's seismic risk. On April 25, 2015, a M7.8 earthquake struck Nepal, affecting a mountainous area from Gorkha to Solukhumbu. The earthquake killed around 9,000 people and left hundreds of thousands homeless. Building collapses during this earthquake sequence were dominated by failures of aging unreinforced masonry buildings and weak vernacular concrete frames. Even though the earthquakes occurred in the dry season, many people were also killed by landslides (Build Change, 2015; Hashash *et al.*, 2015). Review of damage photos shows numerous cases of collapsed hillside concrete frames with well-known vulnerabilities such as weak stories, which may cause collapse before the onset of other hillside failure modes, such as foundation pull-out (Lizundia *et al.*, 2016). Despite these of major damage to hillside structures at some sites, Ram and Junji reported that hillside structures did not experience more damage relative to other building types (2015). Overall, a lack of consensus exists as to the extent of damage to hillside structures with stepped foundations from this earthquake.

More recently, on January 3, 2016, a magnitude 6.7 strike-slip earthquake struck near Imphal, India (USGS, 2016), less than 400 km from Aizawl. Several buildings collapsed from the shaking, while many other structures experienced serious damage and nine people were killed (BBC, 2016). The occurrence of this earthquake event so close to Aizawl heightens the importance of quantifying the seismic vulnerability of the city's building stock and developing recommendations to mitigate damage from future earthquakes in Mizoram.

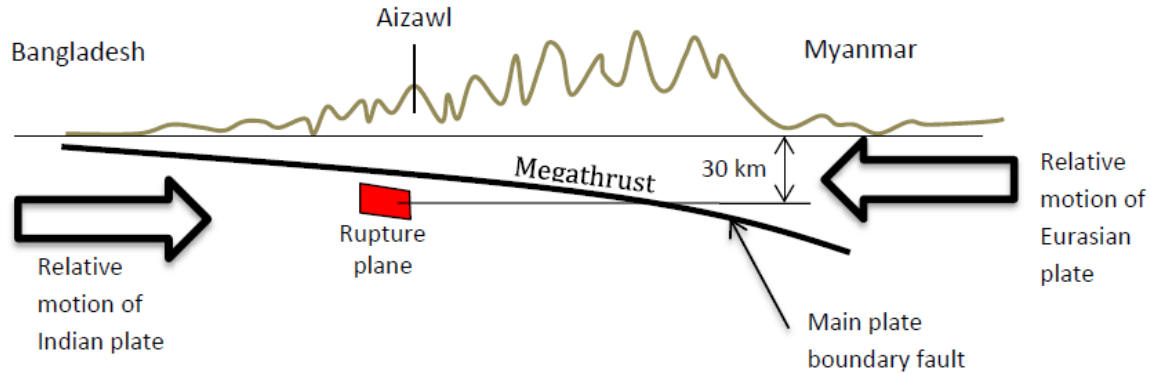


Figure 2. East-west cross-section showing rupture plane expected to cause scenario event from GHI study from GeoHazards International(2014) based on the work of Seeber *et al.*(2013).

1.3 SOCIO-POLITICAL CONTEXT

Aizawl is the capital city of the state of Mizoram, which is bordered to the north by the Indian state of Assam, to the east by Myanmar, and to the south and the west by Bangladesh (Figure 3). The city of Aizawl has seen rapid population growth in recent years, but with limited central planning for the ongoing urban expansion. Until 2007, Aizawl was run by the state government and has only begun to establish its municipal governance over the last nine years. This city of 300,000 people is thus undergoing a time of significant governmental change, during which city leaders seek to establish their own governance structure and policies while maintaining their community's civil and physical infrastructure.



Figure 3. Map of India showing the state of Mizoram and the city of Aizawl.

Aizawl's community leaders are faced with a need to develop new legal and policy frameworks to mitigate future post-disaster losses, before a major earthquake strikes. The Aizawl municipal government is aware that their landslide and seismic risk are issues that can no longer be deferred and, in response, have partnered with the non-profit organization GHI (discussed in more detail below) to develop new land-use and excavation policies to help mitigate some of this risk (J. Rodgers, personal communication, June 2014). Like all growing cities, however, Aizawl faces numerous other daily challenges such as providing clean water and maintaining city roads that require significant organizational and economic resources. Landslide and seismic hazard reduction in Aizawl are long-term planning initiatives founded in efforts to construct new regulatory authorities with distinct areas of jurisdiction and to encourage collaborative institutional operations. In the case of a major earthquake, the challenges of post-disaster recovery for Aizawl would be immense. The city already has limited economic resources to support basic municipal programs; the economic and social losses produced by a severe earthquake could prove catastrophic to the long-term well-being of Aizawl.

1.4 PREVIOUS SEISMIC RISK ASSESSMENT

The impetus for my involvement in Aizawl came from a field study with the non-profit organization, GeoHazards International (GHI), in Aizawl. The mission of GHI is to reduce loss of life and socio-economic harm in communities vulnerable to geologic hazards (GeoHazards International, 2015). Since 2012, GHI has worked in Aizawl with municipal leaders to design and implement policy and educational strategies for mitigating against landslide and seismic hazards.

In 2014, GeoHazards International (GHI) released a study of the potential impact of a high consequence, rare earthquake on Aizawl. The report, written by a team of professional engineers, planners, and geologists, details potential economic, structural, and social losses under a M7.0 event that generates a peak ground acceleration of 0.35g in the region (GeoHazards International, 2014; Iyengar *et al.*, 2010). The scenario predicts 14,000 buildings would collapse and that earthquake damage would impair roads, impeding emergency vehicle access and isolating many areas of the city. The death toll is predicted to be as high as 18,000 in the dry season and the magnitude of the losses could increase if the event were to occur in monsoon season, when over-saturated soils make earthquake-induced landslides potentially larger and more deadly.

In order to better prepare for the possibility of a large magnitude, high consequence earthquake event, such as in Gorkha or Imphal, the municipal government and the team leaders in GHI would like to create a more detailed analysis of the vulnerability of the built environment. To these ends, a computational model of a typical building in Aizawl is developed to analyze the building's vulnerability to ground shaking. Finally, a sensitivity study assesses how variations in structural and material characteristics could improve or worsen collapse resistance.

Chapter 2 AIZAWL'S BUILDING STOCK

2.1 FIELD WORK

During a three-week field visit to Aizawl in June, 2014 with GHI, I surveyed typical building characteristics of Aizawl's building stock, as well as features that could contribute to seismic vulnerability during a three week visit in June, 2014. I visited ten different new construction sites to conduct in-person building assessments of local building stock and the common construction practices. I also spent two days at the Aizawl Municipal Office photographing and reviewing municipal building plans for twelve other previous building projects. My data collection concentrated on two neighborhoods near the site of the March, 2014 landslide by the Ramhlun Sports Complex (in the Ramhlun Venthar and Ramhlun Venglai neighborhoods). These neighborhoods line the northeast side of the city; in this area, buildings are predominantly reinforced concrete and Assam-type. A region of approximately one mile in circumference was selected for field surveys because the building typology is considered representative of the city's new reinforced-concrete building stock. The data collection in the field consisted mainly of visual observations of construction sites, but with the assistance of a translator I also conducted informal interviews with six local masons and construction workers, taking written notes of responses.

For each building surveyed, it was important to gain information about both the building configuration and the on-site construction practices, as both can contribute to structural vulnerability during a hazard event. Of particular interest were the typical geotechnical construction practices, which previous GHI fieldwork and review of building plans had been unable to determine. At each site, the translator and I approached masons, with the hope of

speaking with foremen/chief builders, and asked whether they were willing to answer some questions about the ongoing construction. At most of the building sites it was not possible to identify the foreman or chief mason, and spoke with whichever worker was available at that time. At each site we consistently asked two questions: “What is the method you use to compact the soil under the footings?” and “To what depth do you dig the foundations?” Due to the informal nature of the interviews we only received three responses about the embedment depth out of ten conversations. One construction crew said that they dig the foundations 8-10 ft., while workers at the other two responding sites told us that they always dig 6-6.5 ft. (around 2 meters deep), which is more consistent with notes observed in municipal building plans. The interviews also elucidated that there is not a documented procedure to measure soil compaction and that compaction typically is conducted by hand with a metal rod.

The remainder of data collected came from visual observations of construction practices at the sites, such as whether retaining walls were placed against the slope, whether a grade beam was used at the ground floor, and the dimensions of columns and beams. Our interviews offered insight into common misconceptions workers hold about building design and helped us understand the tight economic constraints that impact building design and construction in Aizawl.

2.2 CONSTRUCTION PRACTICES

Numerous factors impact the seismic vulnerability of buildings in Aizawl, especially the challenging geological and topographical context described above, as well as both socio-economic challenges. Another challenge identified in informal interviews with the city engineers and a private architect is the lack of oversight during construction by engineers who design the structures and the masons who construct them. This issue affects both public and private construction projects in the city. Field observations noted that most new construction projects meet building code

requirements such as by using appropriate stirrup spacing within a distance of $d/4$. However, conversations with engineers at the Aizawl Municipal Council suggested that most buildings are designed only for gravity loads, not seismic design based on the code response spectrum.

In addition, the municipal government has limited funding for continuing education to offer training in seismic design principles for city engineers. Since 2007, the Aizawl Municipal Council has mandated ductile detailing for all new buildings to improve seismic performance of RCC frames (GeoHazards International, 2014), but there is little to no enforcement of this requirement. Nevertheless, field surveys by GHI suggest that the city has seen relatively high compliance rates with ductile detailing code provisions, due to efforts by local architects and engineers to train masons in ductile detailing and to the propensity of private masons to copy construction practices at government sites. Observations by GHI consultants conclude that most existing RCC buildings, however, are still older, non-ductile frames.

With respect to market-based factors, misconceptions by masons that engineers over-design the structures without cost consideration leads many workers to reduce steel area in beams and columns. The construction industry is further limited by the high-price of land development, which often leads to incremental construction practices, discussed in more detail below. Around the world, incremental or progressive construction constitutes 50 to 90% of construction in developing communities. In many cases, the greatest barrier to actual construction is financing, due to a lack of banking and mortgage sectors for construction (Greene & Rojas, 2008). Self-assisted housing is a common form of incremental construction where the construction and financing is carried out mainly by the building owner, allowing an owner to first obtain a plot and to demarcate property lines before construction begins, while slowly raising small amounts of capital to complete each story of the building (Bredenoord & van Lindert, 2010). Despite the

economic benefits of incremental construction, these practice can lead to corroding rebar and weathered concrete, before construction is complete.

2.3 BUILDING MATERIALS

The results of my fieldwork in Aizawl suggest that concrete grade is typically 2,900 psi (M20) based on an admixture of about 1:1.5:3 (cement to sand to coarse aggregate), while the reinforcement steel typically has a yield strength of 60,000 psi (metric grade F415). A water/cement ratio of 0.55-0.60 is assumed in design, and the on-site interviews suggest that most engineers believe that this recommendation is followed in practice. However, conversations with local masons indicate that many workers find that putting more water in the concrete mixture makes it easier to stir and to place formwork. Higher water/cement ratios may contribute to a loss of strength once the concrete has set. Given the high cost of renting or owning a concrete mixer, concrete is often mixed by hand; imprecise mixing can reduce the quality or strength of concrete and affect curing time.

2.4 BUILDING DESIGNS AND CHARACTERISTICS

Buildings in Aizawl consist primarily of three types: “Assam-type,” “Semi-permanent,” and reinforced concrete (referred to throughout South Asia as “reinforced cement concrete” or “RCC”). Assam is traditional light timber building frame. Semi-Puca buildings have a concrete frame with wood walls and floors, or sometimes brick infill walls. RCC uses a concrete frame with brick infill walls, as shown in Figure 4. Forty-seven percent of existing buildings in Aizawl are RCC construction, based on a survey conducted by GHI from 2013-2014 (GeoHazards International, 2014). Compared with construction elsewhere in India, many newer buildings in Aizawl have weaker infill walls, often constructed only a single brick wide or as “brick-on-edge.” The brick-

on-edge practice sometimes is employed to maximize floor space by moving exterior walls onto cantilevers outside of frame lines, but chiefly occurs due to a belief that lighter buildings perform better in earthquakes by placing less demand on the weak slopes. Aizawl's steep slopes require most buildings to be constructed with stepped foundations, where individual footings rest on a flat surface, but "step" up the hillside like a staircase at every or every other column line. This study analyzes Aizawl's most common building configuration: RCC frames with stepped foundations.



Figure 4. Typical residential building in Aizawl with reinforced concrete frame and masonry infill.

The average story height of RCC frames in Aizawl ranges from 10 to 11 ft. The majority of new buildings use the same area of column and beam longitudinal reinforcement at every floor (#5-#7 bars [Imperial sizes], with metric-sized bars smaller than Imperial size #3 bars in the transverse direction). According to our interviews with municipal engineers, a lack of structural engineers working in the building permit department constrains the team's time for detailed building and analysis. As a result, it is common for engineers to simplify designs by selecting beams and columns with the same size dimensions from ground to roof. In addition, most new buildings were observed to have a grade beam level with the ground floor slab. Stirrup spacing was observed in some cases to be greater than Indian building standard requires (no greater than $d/4$ or 8 times larger than the smallest diameter of longitudinal reinforcement steel), although most

stirrup placements appeared to have the necessary 135° hook (BIS, 2002). The national Indian building code (referred to here as BIS) requires that the maximum longitudinal reinforcement ratios (the area of steel divided by the area of the column face) for seismic detailing should be no greater than 0.025 and building plan typically specify reinforcement ratios between 0.02-0.027, but field observations suggest that these values vary greatly in the field, depending on the diameter of longitudinal reinforcement used.

A misconception among many construction workers is that more steel is needed for slabs than is specified in design drawings, but that as-designed beam and column reinforcement is excessive. Therefore, masons sometimes purposefully place less rebar than specified in beams and columns. Slab design typically calls for #3 (#10 in Metric sizing) bars spaced 3.94-7.87 in (100-200 mm). In the field, slab steel is typically placed every 2.95-3.94 in (75-100 mm), with concrete cover of 0.98 in (24.9 mm). Due to the demand for a limited supply of space in Aizawl, many building owners feel pressure to lay claim to a plot as soon as possible (J. Rodgers, personal communication, June 2014). Due to financing challenges, half-completed construction sites are abundant throughout the city: foundations are dug only when ample money is obtained to initiate construction. When additional funding is acquired, placement of structural members and rebar can begin. Chapter 3 discusses the socio-economic roots of incremental construction in more detail.

2.5 FOUNDATIONS AND RETAINING WALLS

Figure 5 shows a typical foundation column. Depth to bedrock varies throughout the city and can be up to 60 ft. deep. Given the lack of economic resources for more complex geotechnical testing, engineers make assumptions about the bearing capacity at each site. Average bearing capacity ranges between 36 and 51 psi (250-350 kN/m²) (PWD Mizoram, 2010). Field reconnaissance

suggests that there is no standard practice for compaction, other than tamping with a heavy rod or log, nor is the expected soil bearing capacity used in design well-documented.

Foundations are most typically spread footings. Footing length and depth (dimensions of the square footing resting on the ground) ranges from 3.3 to 6.6 feet (1-2 m), but regardless of building height, the embedment depth of the footing is typically 4-6 ft (1.23-1.8 m). Some structural drawings specify top and bottom layers of footing reinforcement, typically #5-7 bars. In practice, however, it is most common to see only a single, bottom layer is placed. Retaining and foundation walls against the slope are constructed after column concrete is poured. These foundation walls are most often comprised of cut stones two wythes deep, with weep holes. In most cases, retaining walls are constructed on a slight slope to help hold back the earth behind the back wall, and are considered separate from the structural system, thus removing any downslope weight on the back wall of each bay.

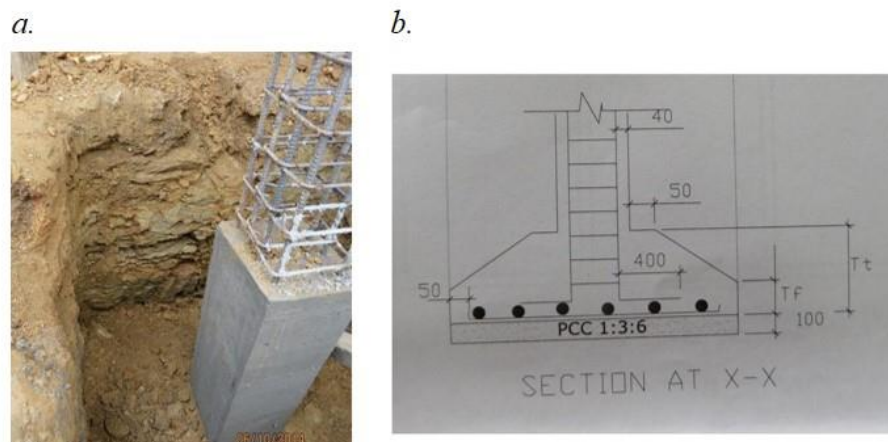


Figure 5. (a) Typical foundation column excavation and (b) building diagram for spread footings (diagram reproduced with permission of Aizawl Municipal Council).

Chapter 3 LITERATURE REVIEW

3.1 HILLSIDE BUILDINGS

This section describes the findings of previous studies of hillside buildings, in terms of structural configuration and performance under static and dynamic loads. Previous research on the seismic vulnerability and performance of hillside buildings in developing communities informs this study, and suggests the need to create more robust structural and geotechnical models to capture important characteristics of the buildings and structural response.

Paul and Kumar (1997) studied slope stability when hillside buildings are placed atop them. They found that the overall safety and stability of a slope depends on the stability of the soil, not necessarily on the building design. If the soil is weak and unstable, even a strongly-sound building can experience collapse. A significant conclusion of their static and dynamic analyses of different building configuration was that heavier building mass should be placed upslope to help stabilize the building under dynamic loading. In addition, they suggested that the stability of a slope under building loads could be increased by employing a deeper foundation embedment. Finally, they also recommended that foundations under columns with the same embedment depth should be placed in one continuous strip instead of individual footings.

Von Winterfeldt *et al.* (2000) assessed potential failure mechanisms for hillside structures, based on damage reconnaissance after the 1994 Northridge earthquake. During the Northridge event, many hillside homes performed well, but some were seriously damaged. In particular, a frequent observed failure was separation of the foundation and structural systems. The study

defined two types of hillside structures: upslope and downslope. Upslope buildings are constructed on ground that slopes up and away from the street, while downslope buildings are constructed on ground that slopes down from the main street. Downslope buildings are more likely to be situated on stepped foundations. Finally, the report suggested that in addition to the foundation type of hillside buildings, the structural response also depends on whether earthquake shaking occurs primarily across or down the slope. The report provided retrofit suggestions for existing hillside buildings to avoid future earthquake damage. The recommended retrofit approach is the make connection between a building and its upslope foundation as strong as possible to reduce risk of it disconnecting under earthquake shaking.

Birajdar and Nalawade (2004) studied the seismic vulnerability of general stepped building configurations, suggesting that hillside buildings are irregular (in both the vertical and horizontal directions) and are torsionally coupled. The study analyzed three building configurations on flat and sloped ground and assumed the foundations were fixed. Their research suggested that when applying an earthquake force along the slope, a much higher shear force developed in the upslope columns, compared with downslope columns. By comparison, for an earthquake force applied across the slope, they observed high possibility of accidental eccentricity at each floor, but with small variation in shear forces between the different building configurations.

Huang (2005) investigated the contribution of bearing capacity failure to seismic instability of retaining walls placed along a slope. This study determined that the angle of friction of the soil has a large influence of soil stability and shear strength during ground accelerations. When assessing structural displacements caused by seismic loading, however, the influence of the friction angle on slope stability is less significant for shallow-sloped hills than for steep slopes. In

addition, less dense (or loose) soil under foundations also amplify vertical and horizontal displacements during ground accelerations.

Both Birajdar and Nalawade (2004), and a similar study by Singh *et al.* (2012), found that shorter columns on the upslope of hillside buildings typically carry the majority of shear forces in a structure. The loading demand on these columns is often much higher than their shear capacity and leads in many cases to shear-dominant failures. Experimental testing and finite element modeling by Wu *et al.* (2014) of the quasi-static performance of multi-story Chinese hillside buildings with stepped foundations also demonstrates that collapse in these structures typically initiates with failures in upslope, ground-story columns.

Kharel *et al.* (2014) considered how displacement of response varied along building height and examined the effect of including beam-on-nonlinear-Winkler (BNWF) foundation models to represent foundation flexibility. Using a beam-on-nonlinear-Winkler foundations included consideration of soil flexibility, thereby decreasing the slope of the building pushover curve. In addition, this modeling approach led to greater displacements under dynamic loading that resulted from the added flexibility in the soil-foundation-structure-interaction. Analysis by Farghaly (2014) hillside, reinforced concrete buildings in Doronka, Egypt provides further insight into modeling choices for the building types considered here. Farghaly suggested several requirements to improve foundation design on slopes, including consideration of the soil capacity around the foundation, ensuring overall slope stability, and whether application of loads will result in acceptable total or differential settlement. The study advocated for using finite element modeling approaches to represent soil behavior due to the complexities for force-deformation response.

3.2 SOIL-STRUCTURE-INTERACTION MODELING

The findings from the previous studies of hillside buildings emphasized the importance of considering soil-structure-interaction in building models. For stiff structures, ignoring foundation deformation can lead to unrealistic characterizations of damping and modal frequencies, both of which can further lead to mischaracterization of seismic performance (Gajan, Hutchinson, Kutter, & Stewart, 2008). Moreover, deformations that occur at the interface between the soil and foundation can change the overall soil-structure-foundation flexibility. Previous guidelines to analyze these systems have simplified this problem by representing the systems as elastic impedance functions to describe the stiffness and damping, but these approaches do not describe the nonlinear behavior of the soil-structure interactions. Some examples of nonlinear behavior that can occur are gap formation between soil and foundation, energy dissipated by hysteretic movement, and rocking or sliding of the foundation.

There are two common approaches to modeling soils and soil-structure-interaction: beam-on-nonlinear-Winkler-foundation (BNWF) models and contact interface models (CIM) (Gajan, Raychowdhury, Hutchinson, Kutter, & Stewart, 2010). BNWF models use independent zero-length soil elements to capture the interaction of the soil and footing, and create elastic beam column elements to represent structural footing behavior. Dynamic BNWF models fall in the category of dynamic p-y methods, which are a simplified approach to uncouple soil and structure, where $p(x)$ is the resultant soil reactions over the length of the foundation column and $y(x)$ is a function representing the foundation column deflection (Pando, Ealy, Filz, Lesko, & Hoppe, 2006). In general, nonlinear p-y behavior is characterized as consisting of elastic, plastic, and gapping p-y components used to build element backbone curves representing soil and the soil-

foundation interface. Typical BNWF model response in general matches structural response under earthquake shaking, although sometimes slightly underestimated peak superstructure displacements. In addition, calculated and recorded structural response from a model calibration study was affected strongly by the frequency of the earthquake ground motions (Boulanger, Curras, Kutter, Wilson, & Abhari, 1999). In *OpenSEES*, the BNWF model is currently available only for two-dimensional analysis and constructs one-dimensional elastic beam column elements with 1-D soil springs to simulate vertical load-displacement, horizontal passive load-displacement (against the side of a footing), and horizontal shear-sliding (at a footing base). Vertical springs are distributed along the base of footings in this model to capture gapping, uplift, and settlement of the foundation (Gajan *et al.*, 2008, 2010).

In contrast, CIM combines a rigid footing and soil beneath the footing into a single macro-element. The model develops constitutive nonlinear relations between cyclic loads and displacements for rigid shallow footing systems and can capture formation of gaps between footing and underlying soil during cyclic loads. One advantage of the CIM approach is that, unlike in the case of BNWF models, this method couples the moment, shear, and vertical load capacities of a soil-footing system (Gajan *et al.*, 2008, 2010). Comparing the two models, the BNWF directly capture behavior of shallow footing based on user inputs for strength, while CIM assumes a rigid footing. Both models are intended to provide simple application within *OpenSEES* and both can capture complex moment-rotation behavior that comes from foundation sliding and settlement.

Chapter 4 CASE STUDY BUILDINGS

4.1 CONTROL BUILDING DESIGN

Based on field observations and the literature review of structural and geotechnical modeling practices for this building type, a suite of computational models are presented that capture different structural and material characteristics of hypothetical new buildings in Aizawl. The buildings modeled here represent key building characteristics observed in structural plans made available in 2014 by the Aizawl Municipal Council (AMC). The basic building design is an RCC frame, with spread footings on stepped foundations. The study building is six stories, with three bays perpendicular to the hill and three hill-parallel bays, shown in Figure 6(a). Each building has a footprint of 39.4 feet by 39.4 feet (12 square meters). Columns are 10.8 feet (3.3 meters) at every story; beams are 13.1 feet (4 meters). The effective building weight of each building is approximately 300 kips, using a dead load of 113 psf and a live load of 20 psf at each floor. The study considers and models only the structural frame, without masonry infill walls (a reasonable assumption given the limited added strength from the weak walls typically used as in infill in Aizawl). A key design feature is the stepped footings, which step up and back at each column line, and are all embedded at the same depth, 5.75 ft (1.75 m), relative to the soil surface on the slope.

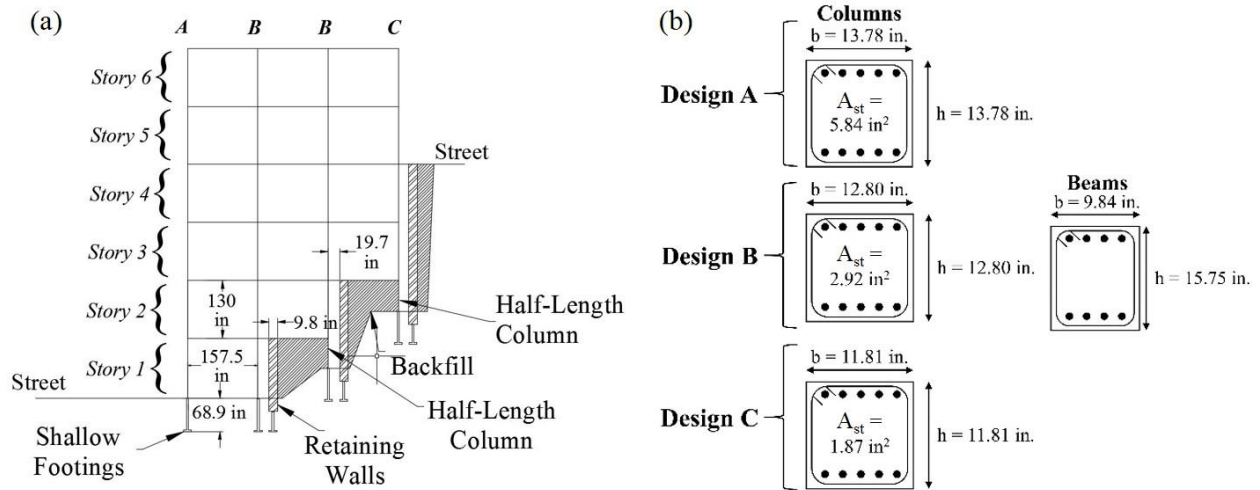


Figure 6. Illustration of control building showing (a) elevation view of building configuration and (b) column and beam dimensions and detailing for case study building (dimensions not to scale).

The first two column lines (C1 and C2) rest on the downslope street level, while the third and fourth (C3 and C4) step up the slope. The base columns on lines C3 and C4 are half the height of the other columns (referred to here as “short” columns). In this study, story numbers are defined beginning at the ground story on the downslope side, *i.e.* “story 1” is the ground story at the bottom of the slope. The retaining walls are not assumed to hold back lateral soil forces on the columns. Thus, any lateral or vertical structural support provided by the retaining walls to the frame is considered negligible, although the weight of the backfill and retaining walls is accounted for when modeling soil capacity. Concrete strength and steel reinforcement yield strength follow AMC building plan specifications (2,900 psi and 60 ksi, respectively). Member dimensions on a column line are uniform over the entire height, but the as-designed downslope columns are deeper and wider than those upslope. Design detail A is used at column line C1, design detail B is used at C2 and C3, and design detail C is used at C4, as presented in Figure 6(b). It is assumed that the building was constructed after 2007, thus meeting national Indian design code detailing requirements (BIS, 2002); the transverse reinforcement uses 0.31 inch diameter bars (#3 Imperial bar size, converted

from Metric #8 bar size) in columns and beams, at a center-to-center spacing of 4 in. The dimensions of the footing are provided in Table 5.

Table 1. Footing dimensions and detailing for case study building.

Footing Width (in)	Footing Length (in)	Footing Depth (in)	Footing Longitudinal Steel (16 mm bars = 0.63 in diam.)	Embedment Depth (in)
70.87	70.87	11.81	12 #5 bars	69.00

4.2 INITIAL DESIGN SENSITIVITY STUDY

Analysis of an archetypical RCC multi-story building will help to quantify the seismic risk of these building types in Aizawl. Model 4 (presented in Table 2) is used as the control design from which structural, geotechnical, and material properties of 16 different building designs are modified. The static analysis results of this sensitivity study will identify design features that most influence the seismic vulnerability of these structures. From the results of this sensitivity study, the modeling parameters and structural design characteristics are refined for a final set of building design variations to evaluate in the seismic risk assessment, based on dynamic analysis.

4.2.1 STRUCTURAL, MATERIAL, AND GEOTECHNICAL DESIGN VARIATIONS

Table 2 presents the structural and material design choices assessed in the first round of the sensitivity study. The first two design variations, building designs 1 and 2, compare changes in structural response from modeling the column-footing connection as either a fixed base or BNWF foundation. Building designs 3 and 4 also compare these foundation models, but with the addition of shear and axial limit state materials at the beam-column joints.

The remainder of the building models examine design variations with respect to structural, material, or geotechnical characteristics. Building design variations 5-7 are used to investigate the significance of the typical column layout found in AMC building plans, where larger column

dimensions are placed on the downslope column lines. Building variation 5 assumes that the largest column dimensions (column section A) at each story are present at all frame lines. Building variation 6 (shown in Figure 7) places uniform column dimensions at each frame line, but with decreasing column sizes at higher stories. In building design variation 7, the order of column dimensions is reversed, such that the smallest column dimensions, column section C, is placed on the downslope side of the building.

Building design variation 8 considers the impact of increased stirrup spacing that does not satisfy code specifications for transverse reinforcement. As was observed during field work, incremental construction practices in Aizawl may cause steel and concrete to weather before construction is complete. Developing representative material models that capture effects of this degradation is beyond the scope of this study. Instead, building variations 9 (lower concrete strength) and 10 (lower steel strength) are proxies for the potential influence on building performance if using lower material quality than specified in design. Building variation 11, enhanced concrete strength, is employed to quantify potential improvement in structural performance from enhanced material quality.

Building design variation 12 (shown in Figure 8) examines how stepped foundations change the response of these hillside structures. In this design, it is assumed that the bearing capacity of the four foundations is the same as for the foundations under column design “C1” in the control building design, ID 4, *i.e.* no effect from backfill or retaining walls on the foundations. To minimize the number of variables altered, the flat foundation design (ID 11) uses the same column configuration as the control building (ID 4). In reality, this type of flat excavated buildings would likely have a symmetrical column layout, to avoid any irregularity in structural dimensions.

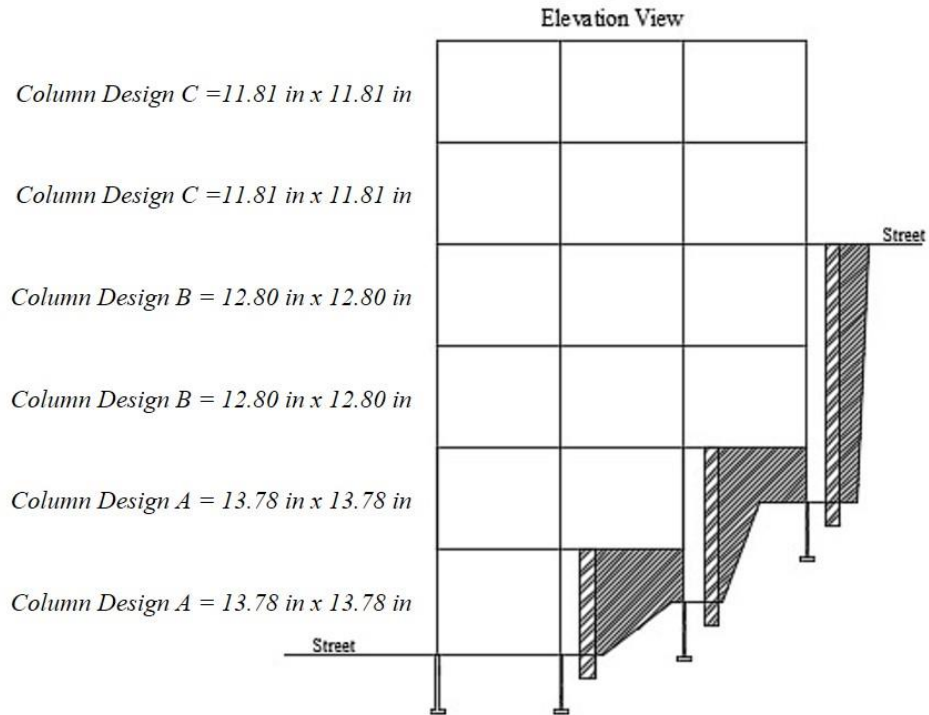


Figure 7. Elevation view of structural variation with different column dimensions at each floor, design ID 6 in Table 2.

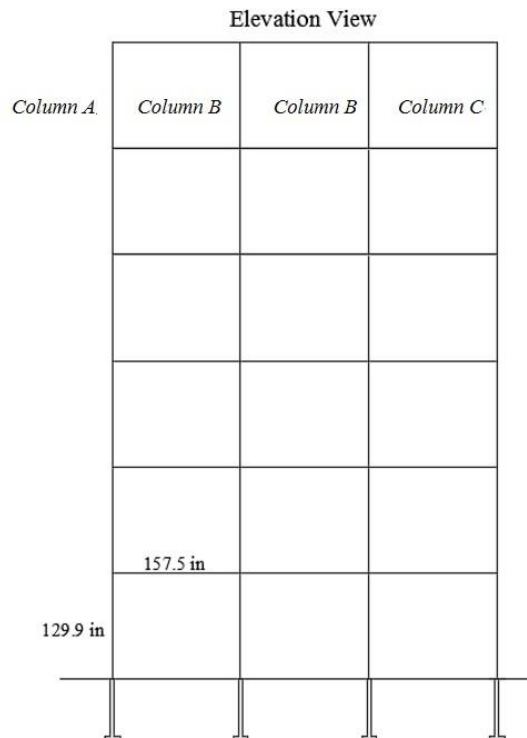


Figure 8. Elevation view of flat foundation building variation, design ID 12 in Table 2.

Table 2. Variations in structural designs.

Building Design ID	Column Sizes	Foundation Type	Shear Springs	Stirrup Spacing	f'c (ksi)	fy (ksi)
1	A, B, C	Fixed	No	Varies	2.90	60.00
2	A, B, C	BNWF	No	Varies	2.90	60.00
3	A, B, C	Fixed	Yes	Varies	2.90	60.00
4	A, B, C	BNWF	Yes	Varies	2.90	60.00
5	A	BNWF	Yes	Varies	2.90	60.00
6	A at Floors 1-2, B at Floors 3-4, C at Floors 4-6	BNWF	Yes	Varies	2.90	60.00
7	C, B, A	BNWF	Yes	Varies	2.90	60.00
8	A, B, C	BNWF	Yes	7 in	2.90	60.00
9	A, B, C	BNWF	Yes	Varies	2.40	60.00
10	A, B, C	BNWF	Yes	Varies	2.90	54.00
11	A, B, C	BNWF	Yes	Varies	3.40	60.00
12	A, B, C	Flat foundation (BNWF)	Yes	Varies	2.90	60.00

The uncertainty in the soil data collected for Aizawl highlights the importance of assessing the differences in structural performance under varying geotechnical properties. The final suite of sensitivity study designs varies parameters important to variabilities in slope stability under seismic loading: the friction angle of the underlying soil and the embedment depth of the shallow footings (Huang, 2005). Table 3 shows the different geotechnical and soil properties assessed, and how these changes influence ultimate, lateral, and passive bearing capacities. This sensitivity study considers first that the friction angle is the same under all footing, and then compares two variations with slightly higher values, to assess how the building response may change with respect to variations in soil shear strength. For comparison, the model for the control building design variation (ID 4) uses $\phi = 24.7^\circ$ and $D_f = 5.75$ ft.

Table 3. Variations in soil and footing properties and effect on bearing capacities.

Building Design ID	ϕ (deg)	D_f (in)	Q_{ult} (kips)	P_{ult} (kips)	T_{ult} (kips)
4.1	27.5	68.9	774	63	219
4.2	30	68.9	1464	69	236
4.3	24.7	78.7	633	73	169
4.4	24.7	98.4	713	114	169

4.3 STRUCTURAL MODELING

Each building variation is modeled in the open-source software platform *OpenSEES* using a 2D frame resisting seismic loads along the slope, because the main interest in this study is quantifying the structural response and vulnerability in the slope-parallel direction. All frame lines are assumed to share the lateral load equally, and so can be modeled with one equivalent frame. The structural members are modeled with 2D nonlinear fiber beam-column elements attached to zero-length shear and axial springs in series to represent flexural response and possible shear and axial load failures of the columns. Figure 9 shows a diagram of the modeled beam-columns. Joints are modeled with elastic joint shear panel springs. 5% Rayleigh damping is assigned to the structure's first and third modes. Geometric nonlinearities are accounted for with a P- Δ transformation (Haselton, Liel, Deierlein, Dean, & Chou, 2011). The impact of masonry infill walls on the response is not considered.

The fiber sections discretize the longitudinal reinforcement and concrete components into fibers, using a Yassin concrete model that captures linear tension softening (Yassin, 1994) and a Giuffr -Menegotto-Pinto reinforcing steel model with isotropic strain hardening (Filippou, Popov, & Bertero, 1983). By integrating the stress-strain behavior of each fiber (Taucer, Spacone, & Filippou, 1991), the fiber elements can capture concrete cracking, onset of yielding, and subsequent spread of plasticity along the length and cross-section of the element (Haselton, Liel, & Lange, 2007). Fiber models are an appropriate choice to model flexural response and allow plane sections to remain plane under deformations. However, comparison of the columns' strengths in flexure and shear demonstrates that, despite following requirements, for ductile detailing, the majority of columns shown in the municipal building plans are still shear critical, *i.e.* they are likely to experience shear failure before flexural failure. Shear failure may be followed by

axial column failure. In order to represent failure mechanisms of these shear-critical elements, zero-length springs are incorporated at the top of each column, with a model developed by Elwood (2004). This model consists of a uniaxial spring that degrades after the detection of shear failure. The limit state model for shear failure detection relates shear demand to drift at shear failure, as a function of the transverse reinforcement and axial load ratios. Elwood also developed an axial spring model to represent column axial failures and loss of column vertical load bearing capacity. Both the Elwood shear and axial limit state models are utilized here.

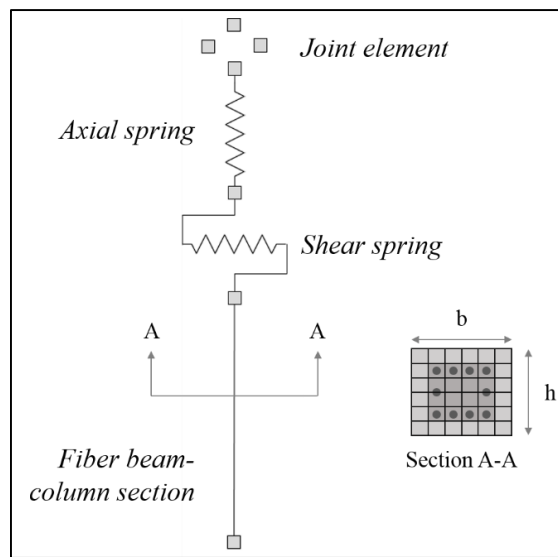


Figure 9. Schematic of beam-column elements, joints, and shear/axial springs modeled in *OpenSEES* (number of fibers shown in cross-section not to scale).

4.4 FOUNDATION MODELING

Previous studies have emphasized the importance of modeling soil-structure-interaction in hillside buildings. One challenge of modeling soil-foundation-structure interaction is that foundations can slide, settle, or rock under dynamic loading. This study takes a BNWF approach to foundation modeling, placing spring elements in combination with soil elements to represent soil-structure-interaction. After review of existing shallow footing models, the *OpenSEES* model *ShallowFootingGen* was selected. This model constructs embedded columns on shallow footings

and connect BNWF footing elements to superstructure beam-column elements with a 2D mesh (Raychowdhury & Hutchinson, 2009). Figure 10 presents an idealization of the BNWF model.

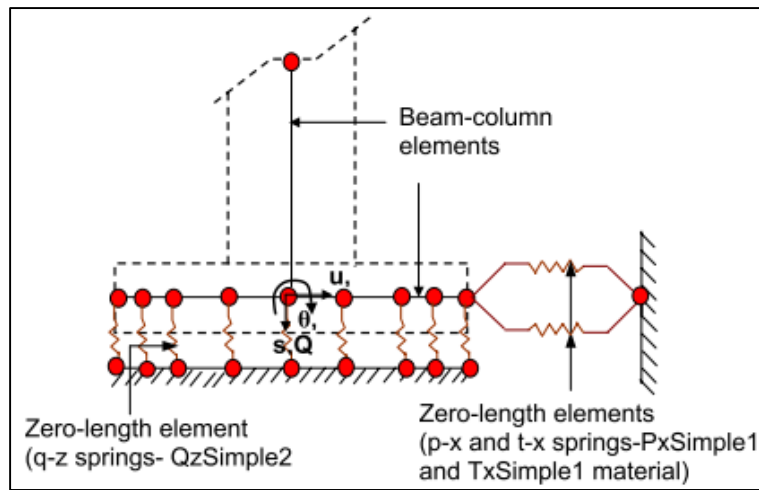


Figure 10. Idealization of beam-on-nonlinear-Winkler foundation model (Raychowdhury & Hutchinson, 2009).

The *ShallowFootingGen* model has been validated with experimental tests. The model simplifies the complex challenge of connecting embedded footings to an above-ground structure, while also effectively capturing the most representative characteristics of footing behavior. Although soil bearing capacity technically changes along the depth of a pile or footing, the model assumes that this effect is negligible for shallow footings and lumps all of the soil behaviors into soil springs connected to the base of the footing. The soil springs connected to the footings are built from three uniaxial materials, to represent: asymmetric hysteretic response caused by the ultimate load on the compression side of the backbone curve and soil's weak tension capacity; passive horizontal soil resistance against the foundation and foundation column, based on equations developed by Boulanger *et al.* (1999) and Matlock (1970); and the frictional soil resistance along the length of the foundation column.

The model currently requires users to specify if the underlying soil is either clay or sand; mixed soils cannot be specified, but users can input specific soil properties, such as shear modulus

and bearing capacity. The study follows the user-defined soil properties approach in an attempt to represent the actual geotechnical conditions in Aizawl. The required user-defined variables are shown in the following tables, along with a short definition of each variable and the actual value used in the model. Table 4 lists the soil model properties, while Table 5 lists the footing variables.

Table 4. Soil properties used for *ShallowFootingGen* model in *OpenSEES*.

Soil Parameter	Description	Value
Soil Type	Either clay or sand (must choose one or the predominate soil type)	Sand
c (ksi)	Soil cohesion	8.68E-05
Φ (deg)	Friction angle	24.7
γ (kips/in ³)	Soil density (unit weight)	6.48E-05
G (ksi)	Soil shear modulus	11.4
ν (%)	Poisson's ratio	0.3
C_{rad} (%)	Radiation damping of soil	0.5
TP (%)	Tension capacity of soil	0.1
β (deg)	Inclination of soil load on foundation with respect to vertical axis (slope of soil above footing)	0°

Table 5. Footing properties used for *ShallowingFootingGen* model in *OpenSEES*.

Parameter	Variable Definition	Value
L_f (in)	Length of footing	76.8
B_f (in)	Depth of footing	76.8
H_f (in)	Height of footing	13.8
D_f (in)	Depth of embedment (from ground level to bottom of footing)	68.9
E_f (psi)	Elastic modulus of footing material	29,000
W_g (kips)	Weight of superstructure on each footing	286
K_x (kip/in)	Horizontal stiffness of footing	505
K_z (kip/in)	Vertical stiffness of footing	88
Rk	Stiffness intensity ratio	2
Re	Footing end length ratio	0.2

The following discussion describes specific details of the selected foundation model variables. According to surveys by GHI geologists, the majority of the underlying soil in Aizawl is saturated sandstone and shale. The *ShallowFootingGen* command is not yet validated for soil mixtures, so the soil is classified for this analysis with the model's *SoilType2* (sand), the dominant soil type in the region. Given that the model does not contain backbone curves for mixed soils, the sand soil type required that the model was input as if it was a cohesionless soil, where $c = 0$, because we wished to study the influence of variance in the soil friction angle (Φ). Future

extensions of this work could explore other soil models that allow for more comprehensive definition of mixed soil parameters.

The angle of soil load inclination (β) depends on the slope of the soil around the footings. This study considers that the soil around the footing makes the foundation rest on a flat surface, even though the slope rises up underneath the building. With this assumption, $\beta = 0$ for each footing. Neither the Aizawl PWD nor the GHI team of external geologists who have surveyed the soil conditions over the last three years provided information on the remainder of the required model variables. As such, the model variables are determined here based on standard geotechnical practice assumptions and equations. The soil modulus of elasticity and Poisson's Ratio are computed from (ATC, 1996; EPRI, 1990), which compiled typical values for soil mechanical properties. Here, the soil is assumed to be loosely compacted and of low to moderate strength. The same assumptions are made for the tension capacity ratio as in the work of Raychowdhury (2009), because $TP = 0.1$ provides the most consistent results when validating the model. Following the recommendations of Madhusudhan and Kumar (2013) a viscous damping ratio is selected of 0.05.

The approach demonstrated in Gazetas (1991) and ATC 40 (1996) is employed here to compute footing horizontal and vertical stiffness. In these calculations, the total footing stiffness is decomposed into horizontal (in both the long and short directions of the footing) and vertical components and then multiplied by embedment depth factors. The footings are square, making horizontal stiffness equal in both directions. These calculations assume that the footing is a rigid plate on homogenous, elastic soil. Tables with the entire suite of equations for these calculations developed by Gazetas (1991) are summarized in both Raychowdhury (2009) and ATC 40 (1996). Finally, the same the stiffness intensity ratio, end length ratio, and vertical spring spacing as in the

ShallowFootingGen example presented in Raychowdhury (2009) are also used here, since those values were already calibrated to provide sufficient spring stiffness along the length of the footing.

The ultimate vertical bearing capacity, Q_{ult} , is calculated based on equations developed by Meyerhof and Adams (1968), which relate the soil friction angle, angle of soil load inclination, the soil Poisson ratio, the soil density, and footing depth of embedment. The factor of safety for the foundations is computed by dividing the resistance of the soil by the demand from the superstructure and backfill on the soil. To calculate the demand on the soil, consider the effect of the backfill behind each footing as the slope rises up to the next level. The first footing, at the bottom of the slope carries only the tributary weight of the frame line above it. The second footing, however, must carry the tributary weight of its respective frame line in addition to the weight of the retaining wall rising to its right (observed in Figure 6a), along with half of the weight of the volume of backfill behind this wall. The third and fourth footings carry the tributary weight of their respective frame lines, the weight of their individual retaining walls, and the combined backfill weight from the half of the backfill volume to the left and right of the footing. Table 6 compares the vertical load resistance of the soil (presented as a stress, in terms of psi) with the load demand on the soil, and the computed factor of safety. In geotechnical engineering, a factor of safety equal to or greater than 3 is considered acceptable: in this model, column A foundation provides adequate support for the vertical demand (*i.e.* factor of safety > 3), but the three other foundations experience a higher demand, such that their factors of safety are significantly less than 3, although demand on the foundations does not exceed their capacity.

Table 6. Vertical resistance versus loading demand from superstructure and backfill and computed factor of safety.

Frame Line	σ_{demand} (psi)	FS
1	30.4	3.3
2	67.7	1.5
3	74.9	1.3
4	50.8	2.0
σ_{ult} (vertical resistance) of each footing is 100.5 psi		

P_{ult} is the passive earth footing resistance along the length of footing that comes from the unit weight of soil, a passive earth coefficient (K_p) and the depth of embedment. The lateral soil resistance of the footing, T_{ult} is based on the classical Mohr-Coloumb failure criteria from the weight of the superstructure on the footing, the angle of friction between the soil and the footing and the footing area (L_f times B_f). These computed soil bearing capacities are compared with data collected for an Aizawl Public Works Department (PWD) survey in preparation for a series of temporary dams around the city in 2010 (PWD Mizoram, 2010). The values from both the PWD field data and from our analytical calculations demonstrate that the soil is weak in passive and lateral sliding resistance, which matches the historical records and field observations of low-strength and high vulnerability to landslides. Table 7 lists the values calculated for Q_{ult} , P_{ult} , and T_{ult} for the original model parameters. In general, bearing capacities are presented as a stress (force over area), but the *ShallowingFootingGen* model requires their input in terms of force (presented here as the stress multiplied over the area of the footing base).

The BNWF model employed here provides a simplified method to consider hillside building soil-structure-foundation interactions. The model also assumes constant and linear soil geometric and material characteristics when, in reality, soil properties change nonlinearly under high shear strains, such as those induced by ground shaking (Seed & Idriss, 1969).

Table 7. Computed values for the ultimate vertical, passive, and lateral soil capacities.

Frame Line	Q_{ult} (kips)	P_{ult} (kips)	T_{ult} (kips)
1	592.5	56.0	137.5
2	592.5	56	257
3	592.5	56	279.9
4	592.5	56.0	200.4

Chapter 5 STATIC ANALYSIS

5.1 INITIAL DESIGN SENSITIVITY STUDY RESULTS

Before assessing the seismic risk of the selected building models, this study seeks to evaluate how the variations in structural, material, and geotechnical characteristics influence trends in strength and ductility. The fundamental periods and base shear values are calculated from static pushover analyses of the *OpenSEES* models. The applied lateral force of the pushover is a triangular distribution. Table 8 presents the results of the pushover analysis for each building design variation described in Table 2 and Table 3. The pushover analysis is first discussed in terms of which modeling features are most important in representing archetypical building conditions in Aizawl. Then, the results are used to determine which structural, geotechnical, and material characteristics of the building design variations modeled here will be most beneficial in comparing the seismic vulnerability of these structures.

Table 8. Fundamental period and maximum base shear values from static pushover analysis

Building Design ID	Max. Base Shear (kips)	T ₁ , (sec)
1	67.48	1.70
2	61.57	2.42
3	39.15	1.69
4	31.12	2.39
5	40.78	2.25
6	38.04	2.39
7	37.93	2.37
8	29.95	2.39
9	28.46	2.52
10	29.93	2.42
11	33.53	2.29
12	29.35	3.08
4.1	30.73	2.45
4.2	39.14	1.69
4.3	30.36	2.29
4.4	30.37	2.29

5.1.1 EFFECT OF BNWF MODEL AND SHEAR AND AXIAL SPRINGS

Model convergence was a persistent challenge throughout the analysis stages. The strain-softening behavior of force-based fiber elements can cause deformations to localize at a single integration point, which disrupted calculation of an objective member response at the onset of shear or axial failure in an element. The modeling approach implemented here did not regularize the fiber beam-column elements, nor was the number of fibers in each cross-section optimized. Both of these changes to the modeling procedure could have significantly improved member response under the applied pushover load distribution (Scott & Hamutcuoglu, 2008). Despite the difficulties in convergence of member response, the results are still considered representative of the overall desired modeling properties and are useful in terms of relative comparisons within this study.

Figure 11 compares the pushover results for building design variations 1-4, the fixed base and BNWF base variations, with and without shear springs. The fixed base models (1 and 2) produce lower maximum base shear values and lower T_1 values than their BNWF foundation counterparts (models 3 and 4) because modeling the foundations with the BNWF models increases the overall flexibility of those models. The introduction of the shear and axial limit state springs (models 2 and 4) decreases maximum base shear strengths and increases yield story drift ratios, because the inclusion of these material springs introduces more realistic failure mechanisms.

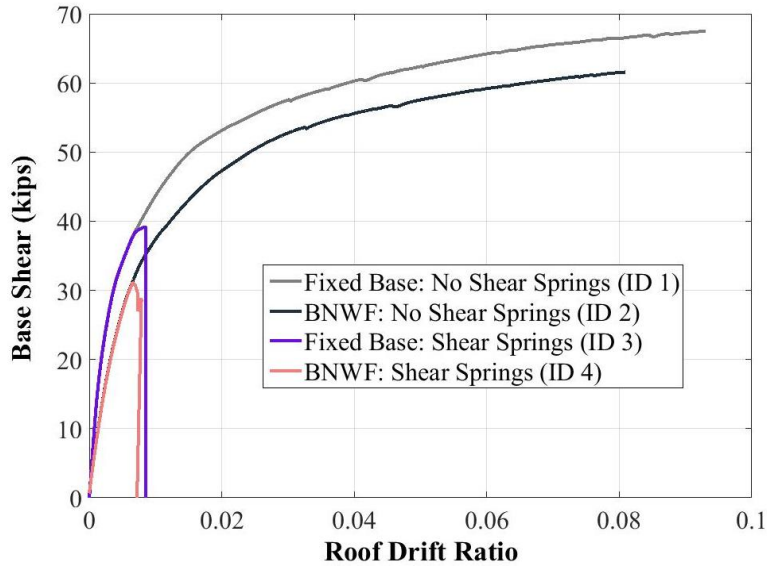


Figure 11. Static pushover results for building design variations modeled with fixed base and BNWF, and with and without shear springs in columns./

5.1.2 EFFECT OF HILLSIDE SLOPE

Few previous studies of pushover analyses for hillside buildings have referenced which direction the lateral load distribution is applied along the slope. The unsymmetrical configuration of these buildings, due to the stepped foundations and placement of short columns, means that lateral forces distribute differently throughout a building depending on whether the pushover load is applied into the hill (upslope) or away from the hill (downslope). Figure 12 compares the pushover results for building design 4 when the load is applied in the upslope and downslope directions. The model fails at a much higher drift ratio when the pushover is applied “out of-hill,” *i.e.* downslope. This trend occurs because the larger downslope columns are able to carry larger loads from the compressive forces of overturning, compared to when the load is applied “into the hill,” *i.e.* upslope, and the smaller upslope columns are required to carry the majority of the lateral pushover load. For the remainder of this study, most results are compared with pushover loads applied into the hill, representing the weakest direction for lateral force distribution in these models.

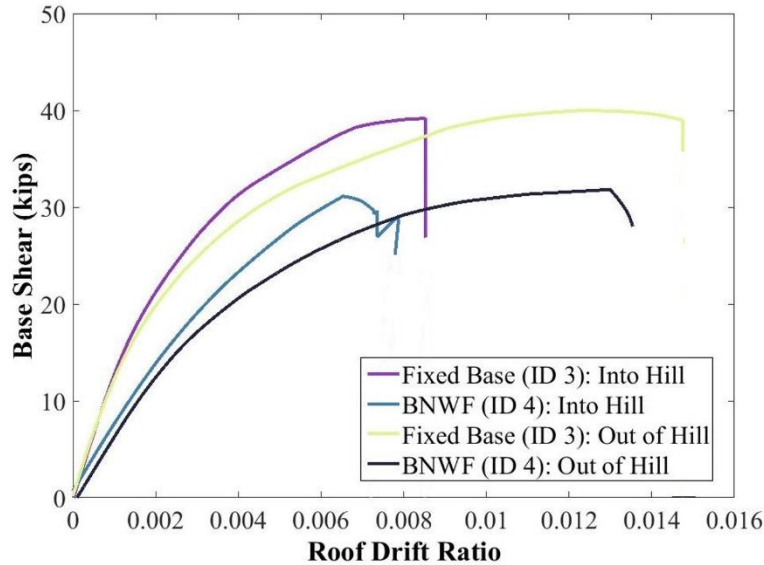


Figure 12. Comparison of pushover results into (upslope) and out of hill (downslope) directions.

Figure 13 compares how the pushover of the stepped foundation design (ID 4) varies from that of the flat foundation model (ID 12). The flat foundation model demonstrates a slightly lower maximum base shear than the stepped foundation model (29.35 kips compared to 31.12 kips). However, the models vary greatly in terms of ductility. In the case of the building design modeled with flat foundations, failure is observed at a roof drift ratio of approximately 1.3%, compared with around 0.6% for the control building design modeled with stepped foundations. The use of full-length columns in building design 12 increases that structure’s overall ductility. The enhanced ductility capacity at each story of this flat foundation building variation contributes to its ability to resist larger deformations before failure. The control building design (ID 4) has a slightly higher maximum base shear than the flat foundation building, due to the additional lateral support provided by the underlying hillside for the stepped foundations design.

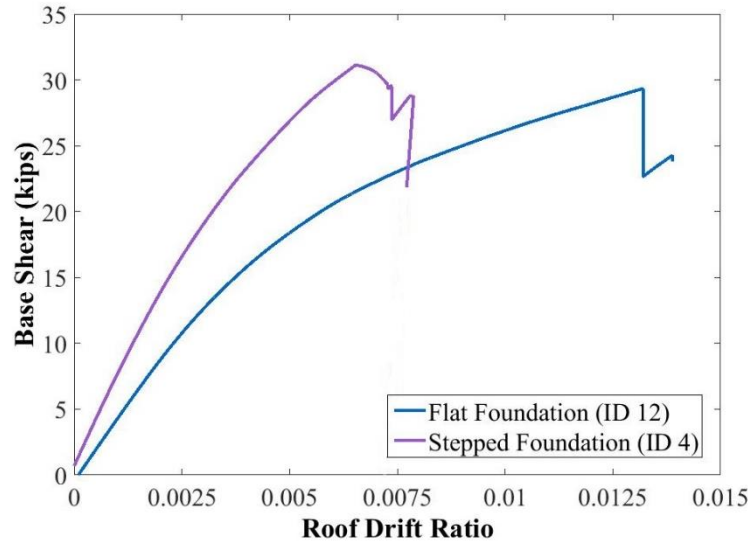


Figure 13. Pushover comparison for flat foundation vs. stepped foundation models.

5.1.3 EFFECT OF STRUCTURAL AND MATERIAL DESIGN VARIATIONS

The remainder of the results are presented with respect to building design variations modeled with the BNWF and with shear and axial limit state materials. These modeling parameters most closely represent the real structural and material characteristics of existing reinforced-concrete, hillside buildings in Aizawl.

Varying the structural member configurations exhibits large differences in both the onset of shear failure and ultimate yielding, as shown in Figure 14. Building design variation 5, with the largest column dimensions (column design A) at all frame lines, demonstrates the highest maximum base shear of the buildings modeled in this comparison group. Decreasing the column size at each floor (but keeping the same member sizes at every slope-parallel (along the hill) frame line on a floor) in building design ID 6, results in a higher maximum base shear and higher roof drifts before yielding (*i.e.* improved ductility capacity) than the control building variation. Under the static pushover loads, reversing the direction of the columns (placing the smallest column dimensions downslope) in building design 7 significantly increases the maximum base shear and

yield drift over the control building, because distribution of forces changes with the placement of larger column dimensions upslope. The results presented next Chapter 6 suggest that the relationship between structural performance and column configuration may depend on whether when a building is subjected to static or dynamic loads. Increasing the stirrup spacing in building design variation 8, selected to mimic real cases observed in Aizawl, exhibits yielding at a low roof drift ratio of around 0.006 inches, and a maximum base shear slightly lower than that of the control building, indicating significant impacts on ductility and lesser effects on strength.

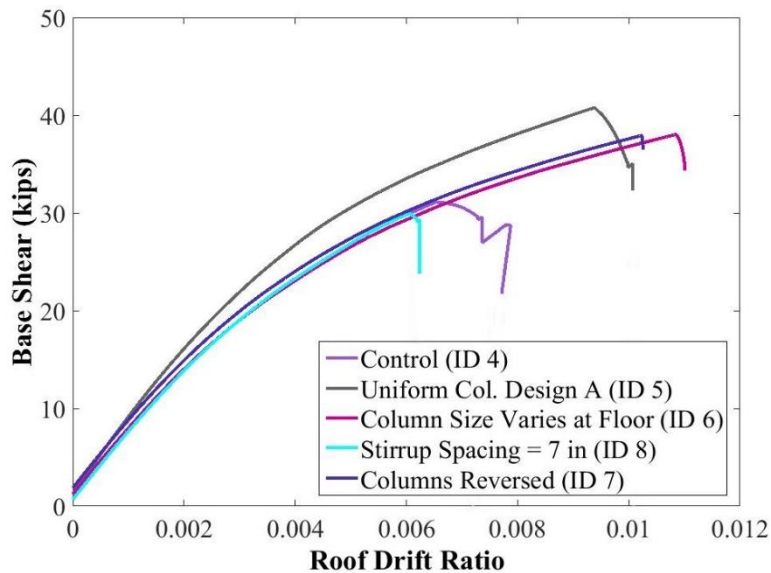


Figure 14. Pushover results for variations in structural configuration.

Analysis of the sensitivity study design variations is expanded to examine the effect of the column configuration by considering both the direction of the pushover load (into and out of the hill) and the column location (smaller, design C, or larger, design A, columns upslope), *i.e.* building design 4 compared with building design variation 7. In both orientations of load application, placing the larger columns at the top of the hill provide more lateral support and produces higher base shear strength and later onset of yielding (Figure 15).

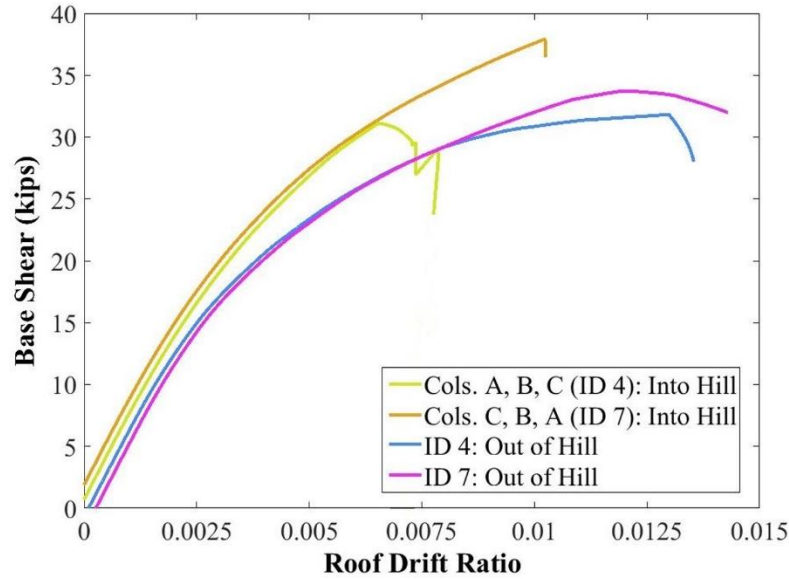


Figure 15. Comparisons of effect of column sizing increasing upslope and decreasing upslope against pushover loading run into and out of the hill.

Varying the material strengths of the concrete and steel produces predictable results: a lower concrete compressive strength (building design 9) or lower steel yield strength (building design 10) decreases base shear strength and results in earlier on-set of yielding than for the control building design (ID 4). In contrast, increasing the concrete compressive strength (building design 11) increases base shear strength and increase roof drift ratio at collapse. Despite these differences in strength and roof drift at yield, these four variations in building design exhibit similar trends in ductility capacity (Figure 16).

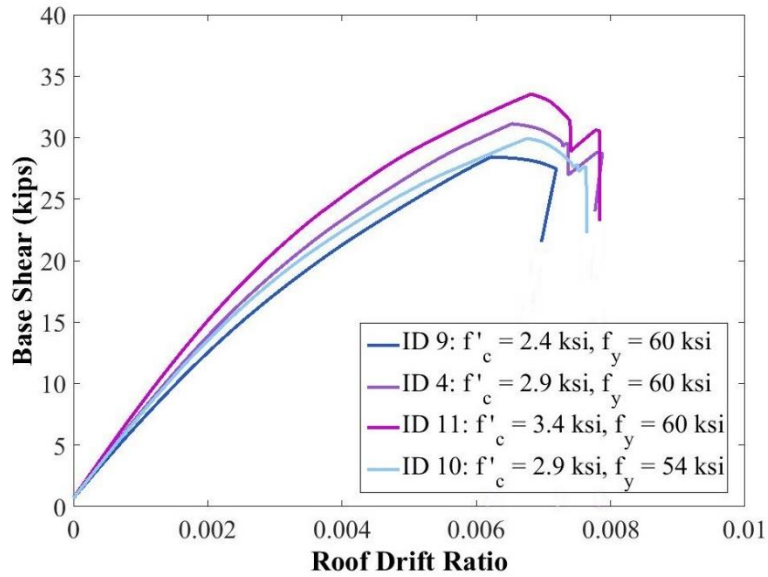


Figure 16. Pushover results for material strength variations.

5.1.4 EFFECT OF FOOTING DESIGN VARIATIONS

Finally, this section of analysis investigates the influence of friction angle or the depth of embedment to the footing on base shear strength and ductility capacity. Figure 17 presents the pushover analysis results for building variations 4.1-4.4, where friction angle (ϕ) and foundation embedment depth (D_f) vary between building models, but are the same under each footing in an individual building variation.

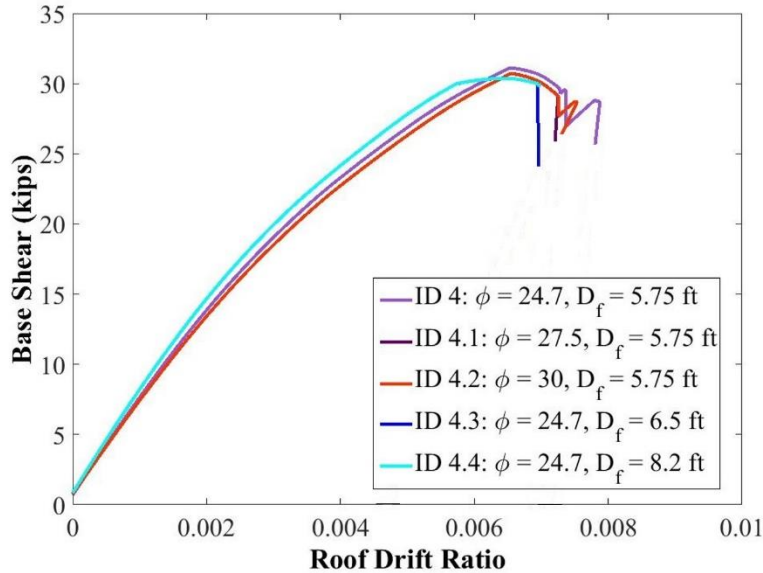


Figure 17. Effect on pushover results from changing foundation model parameters.

The results in Figure 17 suggest that, under the current modeling and lateral loading assumptions, varying friction angle alone within a reasonable range does not have a significant influence on the soil bearing capacity. Similarly, increasing the footing embedment depth does not create a large difference in either ductility capacity or base shear strength. One modeling variation to consider in future analyses of these buildings would be a design that significantly increases the depth of embedment beyond 6 feet (2 meters). Although such an embedment depth would not represent current construction practices in Aizawl, studying this change could suggest potential improvement in construction methods, should it result in improved structural response. Finally, it is possible that the over-simplifications of the footing model employed in this study are not a realistic representation of the effects that changing foundation model parameters impose on superstructure strength and ductility.

5.1.5 CONCLUSIONS FROM STATIC ANALYSIS

The findings from this study informed the selection of modeling parameters and building design variations to consider in the seismic risk assessment. The dynamic analysis will assess building

models with BNWF and fiber element-only models, which were determined in this section to best represent the structural and material responses of archetypical buildings in Aizawl. Given the challenges in modeling the complex soil-structure-interaction and the simplifications made for the footing model, we also choose to exclude the geotechnical model variations from the dynamic analysis study. Upon review of the remaining structural and material variations, it was determined that certain changes to key characteristics of the structural design of building variations (IDs 1-12) described above would better capture the influence of design choices on seismic risk for archetypical buildings in Aizawl. These new building design variations are discussed below.

5.2 REFINED DESIGN SENSITIVITY STUDY THROUGH STATIC ANALYSIS

In the second round of static pushover analysis, the previous building design 4 (BNWF foundation with shear and axial limit state material springs) is again designated as the control building design, but referred to for the remainder of the study as building design I. The suite of design variations considered in the second sensitivity study (presented in Table 9) are: intermediate-sized column dimensions (column design “B”), uniform at all stories and column lines, referred to henceforth as building design II; increased concrete strength ($f'_c = 5,000$ psi), new building design III; increased transverse steel reinforcement (from #3 Imperial bars to #4 bars), new building IV; and a flat foundation building variation with intermediate, uniform column dimensions (design B), rather than stepped foundations, referred to as the new model V. Building design variation II, with column design B, is used to demonstrate the effect of increasing the column size and strength at critical upslope columns, while decreasing column size and strength at the lowest downslope column line (C1). Building designs III and IV evaluate the potential influence of improvements in construction practices and material quality, where the compressive strength in building design III is increased to 5,000 psi because the previous increase to 3,400 psi did not significantly improve

base shear strength or ductility capacity. Building design V is used to examine how stepped foundations change the response and performance of these hillside structures.

Table 9. Structural and material design variations for revised building design variations.

Building Design ID	Column Design	Foundation Type	f'_c (psi)	Stirrup bar size (Imperial)
I (Control)	A, B, C	Stepped	2,900	#3
II	B	Stepped	2,900	#3
III	A, B, C	Stepped	5,000	#3
IV	A, B, C	Stepped	2,900	#4
V	B	Flat	2,900	#3

Table 10 and Figure 18(a) present the pushover analysis results for each building variation. Results for the uniform column building design (ID II) suggest that this configuration slightly increases lateral strength relative to the control building design, at least under static loads. As expected, increasing concrete strength (building design ID III) or transverse reinforcement area (ID IV) increases maximum base shear strength for these buildings. The decreased strength of the flat foundation building design (ID V) is consistent with the static analysis results of the building modeled with a uniform column layout. Building design V does, however, exhibit larger roof drifts (*i.e.* larger deformation/ductility capacity) at loss of lateral strength than the control, due to the placement of full length columns at every column-footing connection.

Figure 18(b) shows the peak interstory drift ratios (IDR) at each column line of the control model. The two upslope short base columns experience much higher IDRs from the pushover than the two downslope full-length base columns. This suggests that a “zippering” failure mode may occur under seismic loads, whereby the capacity of the base column closest to the upslope is exceeded first, followed by sequential downslope failure of the base columns.

Table 10. Results of pushover analysis for revised sensitivity study models.

Building ID	Period T_1 (sec.) ¹	Period-Based Ductility Capacity, μ	Max. Base Shear (kips) ²	Roof Drift At Yield (in/in)
I	2.4	2.3	31.9	0.006
II	2.4	2.2	34.3	0.006
III	1.9	3.9	38.5	0.008
IV	2.4	6.5	49.1	0.026
V	3.1	4.0	30.9	0.014

¹ Period from eigenvalue analysis of nonlinear building models, considering cracked section properties.

² Maximum base shear: maximum base shear per frame line, in units of kips.

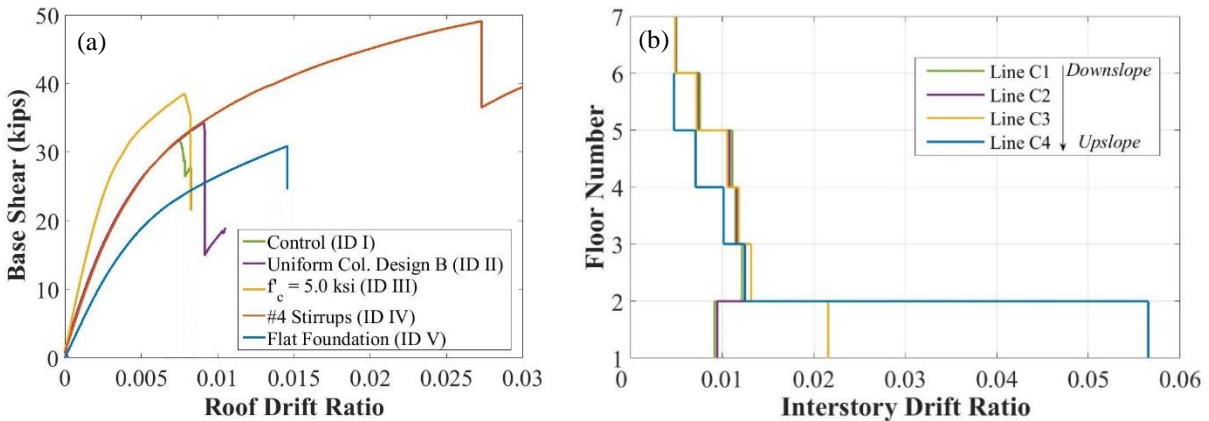


Figure 18. (a) Pushover results for nonlinear models of all building design variations and (b) interstory drift ratios for column lines in control building, where “Floor Number” refers to lowest floor at an individual column line (e.g. 2nd floor is lowest for line C4).

The remainder of this thesis is devoted to the seismic risk assessment of these new building design variations. Chapter 6 describes their structural performance under seismic loading from earthquake ground motions representative of the region in order to develop recommendations for structural engineering decision-making in Aizawl.

Chapter 6 SEISMIC RISK ASSESSMENT

6.1 METHODOLOGY

The objectives of this study are to a) quantify the seismic risk of typical reinforced-concrete buildings in the city of Aizawl (in terms of probability of collapse under scenario earthquake events; and b) identify building characteristics that may either improve or worsen the vulnerability of new hillside construction in Aizawl (based on values of spectral acceleration, peak ground acceleration, and maximum interstory drift at collapse). A suite of ground motions representative of potential earthquake events in the northeast region of India is selected to quantify the seismic risk of these buildings. Then the building's individual and relative seismic risk are assessed using the results of incremental dynamic analysis. This chapter describes the analysis procedure and results and concludes with findings that demonstrate specific vulnerabilities of new and existing buildings in Aizawl, should a major earthquake event occur.

6.2 GROUND MOTION SELECTION

In order to analyze the seismic performance of the selected building designs a list of 44 earthquake events from Mizoram, northern India, Nepal, Bangladesh, and Western China was compiled from databases of historic and recent earthquakes. JWEED, an online database that compiles station and ground motion information, was used to locate seismograms for thirty of these records (Clark & Casey, 2015); acceleration time histories were available for half of the events through SOD, a program to select and process seismogram data for earthquake events (Dept. of Geological Services, 2016). Most of these events, however, came from stations too far from the actual

epicenter to have recorded accelerations large enough to provide useful time history data. Plotting the acceleration time history data for the chosen records revealed only two usable events with peak ground accelerations greater than 0.03g. (Figure 19) shows a plot of the acceleration time history for one of these ground motions, a 2010 event that occurred near the border of Myanmar and India.

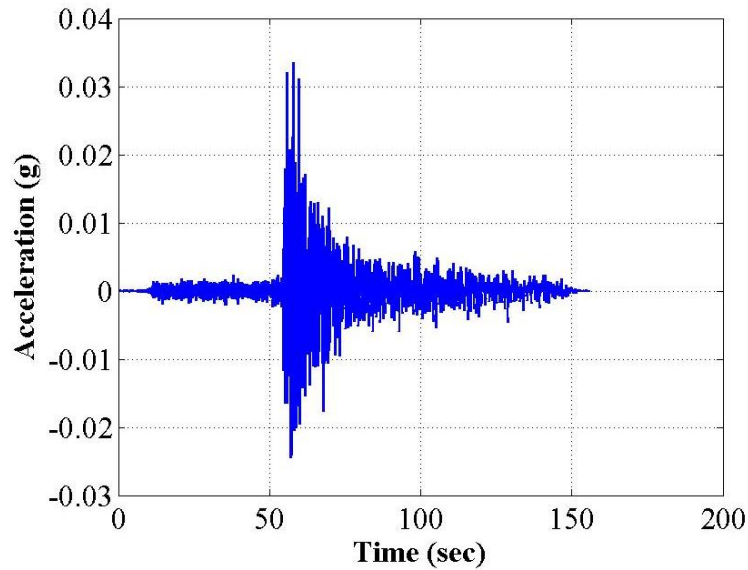


Figure 19. Acceleration time-history plot for India-Myanmar ground motion.

To supplement these two earthquake event records, the information predicted for the GHI scenario earthquake event is used to find additional acceleration time histories from historic earthquakes. The PEER Strong Motion Database provided ten additional ground motions (listed in Table 11) recorded on sites with similar shear wave velocities to Aizawl, between 1,970-2,395 ft/s (600-730 m/s) (determined from the “Custom Vs30 Mapping” tool developed by the USGS), along with the predicted depth to rupture plane (20 km) and magnitude from the GHI study (M7.0) (Ancheta *et al.*, 2013). Given the challenge in obtaining representative, local ground motion records, these ten records are supplemented with the set of 30 strong ground motion records listed in Vamvatsikos and Cornell (2006).

Table 11. Ground motions selected to represent regional seismic hazard in Aizawl.

Earthquake Name	Year	Station Name	Magnitude	Peak Ground Acceleration (g)
Chalfant Valley	1986	Bishop - Paradise Lodge	6.19	0.17
Chi-Chi	1999	CHY035	6.20	0.12
Chi-Chi	1999	TCU084	6.20	0.06
Chi-Chi	1999	TCU089	6.20	0.02
Tottori	2000	OKYH08	6.61	0.23
Tottori	2000	OKYH14	6.61	0.26
Basso Tirreno	1978	Naso	6.00	0.15
Darfield	2010	LPCC	7.00	0.21
Myanmar	2009	BI.DHAK.SHN	5.50	0.39
Myanmar-India Border	2010	BI.DHAK.SHN	5.90	0.33

6.3 DYNAMIC ANALYSIS

6.3.1 INCREMENTAL DYNAMIC ANALYSIS

Dynamic response of the building variations is assessed using incremental dynamic analysis (IDA). In IDA, response spectra are scaled first to a small value of $Sa(T_1)$ and structural response is simulated and recorded. Then, the intensity of the same record is increased at small increments until collapse is observed (Vamvatsikos & Cornell, 2002). This study applies three criteria for collapse: 1) if sidesway results in a peak interstory drift ratio greater than 12%; 2) if shear demand on all columns in a story exceeds the total story shear capacity; and 3) if axial compressive demand of all columns in a story exceeds the total story axial capacity. If no collapse is observed under any of the three criteria, then the analysis is run again at a larger scale factor.

Figure 20(a) presents the collapse fragility curves for all five buildings described in Section 5.2, with ground motion intensities quantified in terms $Sa(T_1)$. Table 12 summarizes median Sa values corresponding to 50% probability of collapse, in terms of both $Sa(T_1)$ and $S(T = 1.0s)$. Normalizing the collapse results to the same period, in this case $T = 1.0$ second, provides a relative comparison of collapse capacity and avoids variations in response due to buildings having different

fundamental periods. This section first discusses the influence of each design variation on the collapse capacities at $Sa(T = 1.0s)$, and then considers how these results compare to the designs of non-ductile buildings in the U.S., and then place these collapse capacities in the context of Aizawl's regional seismic risk.

The uniform column design (ID II) has the lowest median collapse capacity, in terms of $Sa(T = 1.0s)$, of all study building design variations, suggesting that for the building configurations assessed in the IDA, the upslope variation in column dimensions present in the control building is beneficial to lateral load distribution. In the initial sensitivity study, the building design that reversed the order of columns (placing the smallest size at the bottom of the slope) had a higher maximum base shear than a uniform column layout, but an IDA was not conducted for that a building with reversed column design. The results of the static and dynamic analyses for the uniform column layout suggests that future work should investigate the response of a building with a reversed column configuration under dynamic loads, to better understand the relationship in these hillside buildings between column configuration and lateral load distribution.

Using higher strength concrete (ID III) increases the building's stiffness, decreases its fundamental period and results in a slightly lower collapse capacity at $Sa(T = 1.0s)$ than the control building. This finding is consistent with the pushover results for this building (higher base shear strength, lower deformation capacity). The competing strength and deformation capacities of this structure, however, may counter-balance each other in terms of their influence on overall collapse capacity. Increasing the size of transverse reinforcing bars (model IV) significantly improves collapse capacity, due to greater resistance to shear failures. At $Sa(T=1.0s)$ the flat foundation building design variation ID V has a similar median collapse capacity to the control (ID I). Although the deformation capacity of building ID V is greater than that of ID 1, the intermediate

uniform column dimensions of building V do not enhance lateral force resistance and the soil bearing capacity under this building is assumed less than that of the control (*i.e.* the flat foundation case does not consider additional stabilizing pressures from hillside soil loads).

Next, the results are compared to those of Liel *et al.* (2011), which quantifies collapse risk of U.S. reinforced concrete buildings designed before the institution of ductile detailing requirements in the 1970s. The results for an 8-story non-ductile perimeter frame (building design “8P”) in that study are comparable to the building design variations analyzed here, because 8P has a similar fundamental period to our control building. The Liel building design 8P has a median collapse spectral acceleration of $Sa(T_1 = 2.40s) = 0.23g$, only slightly larger than that of our control building, ID I, where $Sa(T_1 = 2.38s) = 0.18g$. This study’s model with increased transverse steel (ID IV) has a collapse $Sa(T_1 = 2.38s) = 0.45g$, compared to that of the 8P design with ductile detailing in Liel *et al.* (0.57g).

Finally, the seismic risk of the study building design variations is quantified relative to a ground motion intensity close to that of the maximum considered earthquake (MCE) for Indian Seismic Zone V (BIS, 2002). The GHI scenario earthquake and the regional MCE correspond to an approximate spectral response of $Sa(T = 1.0s) = 0.40g$, estimated from the expected PGA (0.35g) and the median response spectra curve utilized in the IDA. The collapse margin ratio (CMR) is a common metric to assess collapse capacity relative to a specific seismic hazard level, defined as the ratio of median 5% damped spectral acceleration of collapse level ground motions to the 5% damped spectral acceleration of the maximum considered, or scenario, ground motion intensity (MCE) (FEMA, 2009). Computing the “adjusted collapse margin ratio” (ACMR) helps to correct for the influence on collapse capacity from ground motion frequency content, where the original CMR of each building design is multiplied by a spectral shape factor, based on

fundamental period and period-based ductility following recommendations from FEMA (2009). This adjusted CMR is then compared to recommended values of “acceptable” collapse margins to determine whether probability of collapse at the MCE is less than or equal to 20% given all sources of system uncertainty quantified as recommended in FEMA P-695 (2009), as shown in Table 12. 20% is chosen here as the limit because it represents the upper acceptable collapse probability of modern code-designed US buildings. This analysis computes collapse fragilities based on the expected probability of collapse at MCE, accounting for spectral shape and system uncertainty, and present these fragilities in Figure 20(b). The new collapse probabilities corresponding to MCE are also reported in Table 12. With the exception of ID IV, none of the case study building designs meet the threshold level of acceptable ACMR (1.76) after dynamic analysis, thus indicating that, should the MCE occur, their $P[\text{Collapse} | Sa(T=1.0s)_{MCE}]$ is greater than 20%. Building design variation IV, with increased transverse steel, has an ACMR of 4.96, a far more than “acceptable” collapse margin for U.S. code-compliant buildings.

Table 12. Median values for collapse capacities (presented at $Sa(T_1)$ and $Sa(T = 1.0s)$) and collapse margin ratio and probability of collapse at maximum considered earthquake shaking intensity, accounting for spectral shape and system uncertainty.

Building ID	Median Collapse $Sa(T_1)$ (g)	Median Collapse $Sa(T = 1.0s)$ (g)	Collapse $Sa(T = 1.0s)$ Std. Dev.	Adjusted Collapse Margin Ratio¹	P[Collapse $Sa(T=1.0s)_{MCE}$]
I	0.18	0.47	0.91	1.35	65%
II	0.15	0.32	0.63	1.10	76%
III	0.22	0.44	0.75	1.54	58%
IV	0.45	1.30	0.53	4.96	6.2%
V	0.12	0.46	0.69	1.59	56%

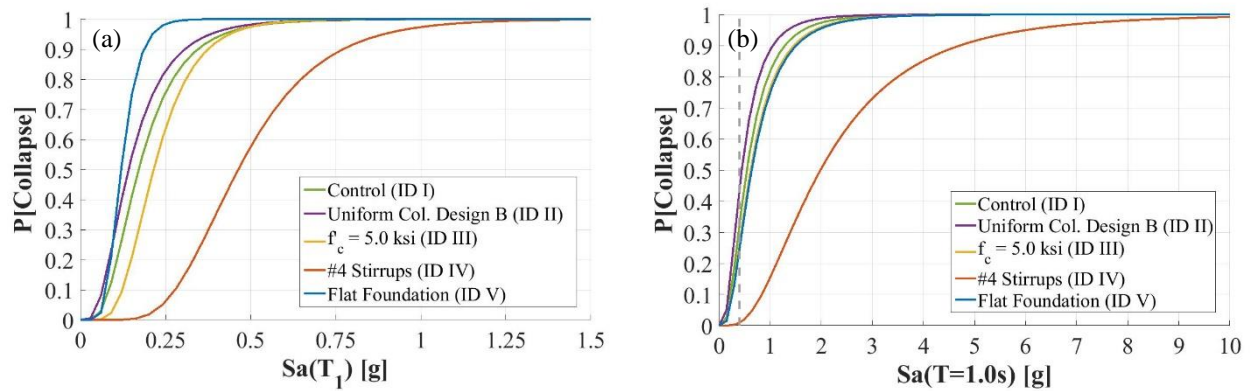


Figure 20. Collapse fragility curves for all five hillside building design variations at (a) $Sa(T_1)$ and (b) $Sa(T = 1.0s)$ adjusted for spectral shape and system uncertainty, where dashed line indicates $Sa(T = 1.0s) = 0.40g$, corresponding to seismic hazard for the maximum considered earthquake in Indian Seismic Zone V.

6.3.2 COLLAPSE FAILURE MECHANISMS

One of the main study objectives is to identify the mechanisms and sequences of failure for hillside buildings with stepped foundations in Aizawl. Examination of the results shows that the failure sequence varies little between the 40 ground motions. Therefore, the failure sequences are mapped from the results of the ground motion record that caused the largest number of column failures for each building. Figure 21 (a) shows a graphical visualization of the combined (shear and axial) column failure sequence for the control building design. As predicted by the pushover results, column failure initiates in an axial mode at the upslope street level base columns, because they are the stiffest and therefore carry large lateral forces. In this damage progression, failure propagates downslope in a sequential “zippering” motion. This pattern progress because, when failure of one column occurs, the subsequent set of downhill base columns becomes the stiffest and must carry more lateral force. As failure propagates downslope through the base columns, the columns in the 2nd and 3rd stories are required to resist an increasing proportion of the lateral load, before these stories fail entirely, causing the entire building to collapse. Exceedance of the 3rd story shear

capacity is predicted to be the most common collapse mechanism under seismic loads for hillside RCC structures with stepped foundations in Aizawl.

Figure 21(b) demonstrates how increasing concrete strength (building design ID III) changes column failure mechanisms, concentrating the majority of failures in the upslope column lines (although the most common collapse mechanisms remains exceedance of shear capacity in the 3rd story). Increasing the transverse reinforcement area (building design ID IV) significantly changes the collapse mechanism; for that building, 40% of the ground motions in the IDA result in sidesway-induced collapse, associated with a flexurally-dominated column failure mechanism.

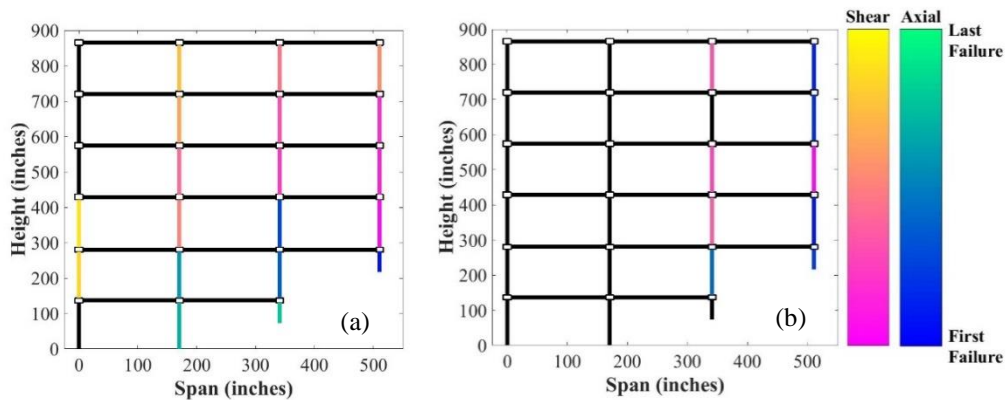


Figure 21. Failure sequence for (a) control building design (ID I) showing upslope to downslope “zippering” associated with axial failures of base columns and (b) for building modeled such that $f'c = 5.0$ ksi model (ID II), meaning failures concentrate in upslope column lines.

Chapter 7 CONCLUSIONS

7.1 LIMITATIONS

The social, economic, and environmental realities of building construction in Aizawl pose significant research challenges to developing models that accurately represent current design and construction practices. This study does not consider material degradation from effects of incremental construction, because including these characteristics requires computational models of changes in concrete-steel bond caused by rust or the onset of concrete corrosion, a complicated task due to the scarcity of empirical data. The foundation model used here is an over-simplification of the complexity of soil-structure-foundation interactions. To better represent these interactions, future work should utilize more detailed foundation models, ideally validated by field testing of foundation pull-out. Possible other improvements to the foundation model could include: using an equivalent linear procedure to interrogate nonlinear soil shear properties under dynamic loading, accounting for differential settlement, and/or employing a fully nonlinear soil model. The results also suggest that if the analysis was continued without convergence issues, all base columns would fail axially (before most upper story columns fail in shear), constituting a global collapse. Finally, this study assessed only hypothetical new structures; further analysis is needed to quantify the seismic vulnerability and identify potential retrofit actions for Aizawl's existing hillside buildings.

7.2 DISCUSSION OF FINDINGS

This study contributes to a growing body of literature that investigates the seismic performance of hillside buildings with stepped foundations. Despite the above-mentioned limitations, the findings

provide insight into the vulnerability of existing reinforced concrete hillside buildings in the northeast Indian city of Aizawl, by quantifying their collapse risk and identifying specific structural failure mechanisms. The results suggest that typical Aizawl buildings have insufficient resistance against lateral loads, but static and dynamic analysis results suggest that uniform column configurations do not enhance lateral strength resistance. Future studies of these building configurations should analyze the seismic performance of a building with the as-designed column layout is reversed, *i.e.* a building design where larger column sizes are placed on upslope column lines. Perhaps unsurprisingly, the control building design variation has a collapse margin below the acceptable level for U.S. code-compliant reinforced concrete buildings at maximum considered earthquake intensities, *i.e.* chance of collapse during MCE shaking is greater than 20%. Static and dynamic analyses demonstrate that the short, upslope, street-level base columns likely will initiate failure, causing sequential downslope “zippering” failure of base columns. Shear failures in the 2nd and 3rd stories are predicted to cause collapse, as they must resist increasing lateral forces after the base columns fail. A sensitivity study demonstrates that larger transverse reinforcing increases collapse capacity and changes the collapse mechanism from weak story to sidesway failure.

Recent earthquakes in Nepal and northeast India foreshadow the risk to life and property posed to the city of Aizawl by a future seismic event. Our findings suggest that to reduce vulnerability under the regional seismic hazard of new hillside RCC buildings in Aizawl, engineers and municipal officials should concentrate mitigation efforts on increasing building shear capacity and ensuring that such measures are enacted during construction. Future research should investigate the influence of specific mitigation strategies, such as strengthening critical base columns, providing greater shear reinforcement, and potentially increasing upslope column sizes.

REFERENCES

- Ancheta, T. D., Darragh, R. B., Stewart, J. P., Seyhan, E., Silva, W. J., Chiou, B. S. J., ... Donahue, J. L. (2013). PEER NGA-West2 Database: PEER Report 2013/03. Berkeley, CA: Pacific Earthquake Engineering Research Center.
- ATC. (1996). *Seismic Evaluation and Retrofit of Concrete Buildings*. Redwood City, CA.
- BBC. (2016, January 4). Earthquake hits India's Manipur state. *British Broadcasting Company News Service*. Retrieved from <http://www.bbc.com/news/world-asia-india-35219069>
- Birajdar, B. G., & Nalawade, S. S. (2004). Seismic analysis of buildings resting on sloping ground. In *13th World Conference on Earthquake Engineering*. Vancouver, Canada.
- BIS. (2002). IS 1893:2002 Criteria for Earthquake Resistant Design of Structures. Bureau of Indian Standards.
- Boulanger, R. W., Curras, C. J., Kutter, B. L., Wilson, D. W., & Abhari, A. (1999). Seismic soil-pile-structure interaction experiments and analyses. *J. Geotech. Geoenviron. Eng.*, 125(9), 750–759.
- Bredenoord, J., & van Lindert, P. (2010). Pro-poor housing policies: Rethinking the potential of assisted self-help housing. *Habitat International*, 34(3), 278–287.
- Build Change. (2015). April 25, 2015--Gorkha earthquake, Nepal. Build Change Post-Disaster Reconnaissance Report.
- Clark, A., & Casey, R. (2015). JWEED. *Incorporated Research Institutions for Seismology*.
- Dept. of Geological Services. (2016). Standing order for data. Retrieved from <http://www.seis.sc.edu/sod/index.html>
- Elwood, K. J. (2004). Modelling failures in existing reinforced concrete columns. *Canadian Journal of Civil Engineering*, 31(5), 846–859.
- EPRI. (1990). *Manual on Estimating Soil Properties for Foundation Design*, Electric Power Research Institute. Palo Alto, CA.
- Farghaly, A. A. (2014). Evaluation of Seismic Performance of Buildings Constructed on Hillside Slope of Doronka Village-Egypt. *ISRN Civil Engineering*, 2014, 1–13.
- FEMA. (2009). Quantification of building seismic performance factors. *FEMA P695*, (June).
- Filippou, F., Popov, E., & Bertero, V. (1983). Effect of Bond Deterioration on Hysteretic Behavior of Concrete Joints. Report EERC 83-19. *Earthquake Engineering Research Center, University of California, Berkeley*.
- Gajan, S., Hutchinson, T. C., Kutter, B. L., & Stewart, J. P. (2008). *Numerical Models for Analysis and Performance-Based Design of Shallow Foundations Subjected to Seismic Loading*. Berkeley, CA.
- Gajan, S., Raychowdhury, P., Hutchinson, T. C., Kutter, B. L., & Stewart, J. P. (2010). Application and validation of practical tools for nonlinear soil-foundation interaction analysis. *Earthquake Spectra*, 26(1), 111–129.
- Gazetas, G. (1991). Formulas and charts for impedances of surface and embedded foundations. *J. Geotech. Eng.*, 117(9), 1363–1381.
- GeoHazards International. (2014). *A safer tomorrow? Effects of magnitude 7 earthquake on Aizawl, Mizoram and recommendations to reduce losses*. Menlo Park, CA. Retrieved from <http://geohaz.org/projects/aizawl.html>
- GeoHazards International. (2015). About Us: Our Mission. Retrieved from <http://geohaz.org/about/index.html>
- Government of Mizoram. (2012). Climate. Retrieved from <https://tourism.mizoram.gov.in/page/climate.html>

References

- Greene, M., & Rojas, E. (2008). Incremental construction: A strategy to facilitate access to housing. *Environment and Urbanization*, 20(1), 89–108.
- Haselton, C. B., Liel, A. B., Deierlein, G. G., Dean, B. S., & Chou, J. H. (2011). Seismic Collapse Safety of Reinforced Concrete Buildings. I: Assessment of Ductile Moment Frames. *Journal of Structural Engineering*, 137(4), 481–491.
- Haselton, C. B., Liel, A. B., & Lange, S. T. (2007). *Beam-Column Element Model Calibrated for Predicting Flexural Response Leading to Global Collapse of RC Frame Buildings*. PEER Report 2007/03. Berkeley, CA.
- Hashash, Y. M. A., Tiwari, B., Moss, R. E. S., Asimaki, D., Clahan, K. B., Keiffer, D. S., ... Adhikari, B. (2015). *Geotechnical field reconnaissance: Gorkha (Nepal) earthquake of April 25 2015 and related shaking sequence*.
- Huang, C.-C. (2005). Seismic Displacements of Soil Retaining Walls Situated on Slope. *Journal of Geotechnical and Geoenvironmental Engineering*, 131(9), 1108–1117.
- Iyengar, R. N., Paul, D. K., Bhandari, R. K., Sinha, R., Chadha, R. K., Pande, P., ... Kanth, S. T. G. R. (2010). Development of Probabilistic Seismic Hazard Map of India, Final Report. *National Disaster Management Authority*.
- Kharel, P., Dhakal, S., & Poudyal, S. (2014). Seismic demand behaviour of low-rise reinforced concrete buildings built on slopes of Kathmandu valley. In *International Symposium Geohazards: Science, Engineering and Management* (pp. 341–347). Kathmandu, Nepal.
- Liel, A. B., Haselton, C. B., & Deierlein, G. G. (2011). Seismic Collapse Safety of Reinforced Concrete Buildings. II: Comparative Assessment of Nonductile and Ductile Moment Frames. *Journal of Structural Engineering*, 137(4), 492–502.
- Lizundia, B., Shrestha, S. N., Bevington, J., Davidson, R., Jaiswal, K., Jimenez, G. K., ... Ortiz, M. (2016). EERI earthquake reconnaissance team report: M7.8 Gorkha, Nepal earthquake on April 25, 2015 and its aftershocks. *Earthquake Engineering Research Institute*.
- Madhusudhan, B. N., & Kumar, J. (2013). Damping of Sands for Varying Saturation. *Geotechnical and Geoenvironmental Engineering*, 139(9), 1625–1630.
- Matlock, H. (1970). Correlation for design of laterally loaded piles in soft clays. In *2nd Offshore Technology Conference* (pp. 577–594). Houston, TX.
- Meyerhof, G. G., & Adams, J. I. (1968). The ultimate uplift capacity of foundations. *Canadian Geotechnical Journal*, 5(4), 225–244.
- MIRSAC. (2005). Hazard Risk and Vulnerability Analysis of Aizawl District. *Mizoram Remote Sensing Application Centre*.
- Pando, M. A., Ealy, C. D., Filz, G. M., Lesko, J. J., & Hoppe, E. J. (2006). A laboratory and field study of composite piles for bridge substructures. FHWA-HRT-0. *Federal Highway Administration*.
- Paul, D. K., & Kumar, S. (1997). Stability analysis of slope with building loads. *Soil Dynamics and Earthquake Engineering*, 16(6), 395–405.
- PWD Mizoram. (2010). Performance evaluation of control of erosion at 3 places (Chhinga Veng, Saron Veng, and Sihpui) Aizawl Mizoram: Final report. *Quality Control Division, Zuangtui: Aizawl, Mizoram, Brahmaputra Board Government of India*.
- Ram, P. R., & Junji, K. (2015). Ground motion characteristics of the 2015 Gorkha earthquake, survey of damage to stone masonry structures and structural field tests. *Frontiers in Built Environment*, 1(23).
- Raychowdhury, P. (2009). *Nonlinear winker-based shallow foundation model for performance assessment of seismically loaded structures*. University of California, San Diego.
- Raychowdhury, P., & Hutchinson, T. C. (2009). Performance evaluation of a nonlinear Winkler-based shallow

References

- foundation model using centrifuge test results. *Earthquake Engineering & Structural Dynamics*, 38(5), 679–698.
- Scott, M. H., & Hamutcuoglu, O. M. (2008). Numerically consistent regularization of force-based frame elements. *International Journal for Numerical Methods in Engineering*, 76(10), 1612–1631.
- Seeber, L., Ferguson, E. K., Ahkter, S. H., Steckler, M. S., Mondal, D. R., Gale, J., ... Goodbred, S. L. (2013). The Brahmaputra delta and its merger into an accretion wedge in advance of the progressive suturing between India and Asia. In *American Geophysical Union, Fall Meeting*.
- Seed, H. B., & Idriss, I. M. (1969). Influence of soil conditions on ground motions during earthquakes. *J. Soil Mech. Found. Div.*, 95(1), 99–137.
- Singh, Y., Gade, P., Lang, D. H., & Erduran, E. (2012). Seismic Behavior of Buildings Located on Slopes - An Analytical Study and Some Observations From Sikkim Earthquake of September 18 , 2011. In *15th World Conference of Earthquake Engineering*. Lisbon, Portugal.
- Taucer, F. F., Spacone, E., & Filippou, F. C. (1991). A Fiber Beam-Column Element for Seismic Response Analysis of Reinforced Concrete Structures. Report UCB/EER-91/17. *Earthquake Engineering Research Center, University of California, Berkeley*.
- USGS. (2015). The Himalayas: two continents collide. *This Dynamic Earth: The Story of Plate Tectonics*. United States Geological Survey. Retrieved from <http://pubs.usgs.gov/publications/text/himalaya.html>
- USGS. (2016). M6.7 – 29 km W of Imphal, India. *Earthquake Hazards Program*. United States Geological Survey. Retrieved from http://earthquake.usgs.gov/earthquakes/eventpage/us10004b2n#general_summary
- Vamvatsikos, D., & Cornell, C. A. (2002). Incremental dynamic analysis. *Earthquake Engineering & Structural Dynamics*, 31(3), 491–514.
- Vamvatsikos, D., & Cornell, C. A. (2006). Direct estimation of the seismic demand and capacity of oscillators with multi-linear static pushovers through IDA. *Earthquake Engineering and Structural Dynamics*, 35(9), 1097–1117.
- von Winterfeldt, D., Roselund, N., & Kitsuse, A. (2000). Framing earthquake retrofitting decisions: the case of hillside homes in Los Angeles. PEER 2000/03. *Pacific Earthquake Engineering Research Center*.
- Wu, Y., Lin, X., Li, Y., & Han, J. (2014). Seismic collapse-resistant capacity of moment frames supported by stepped foundation in mountainous city. *Journal of Building Structures*, 35(10), 82–89.
- Yassin, M. H. M. (1994). *Nonlinear Analysis of Prestressed Concrete Structures under Monotonic and Cycling Loads*. University of California Berkeley.